

**LS3MIP (v1.0) contribution to CMIP6: The Land Surface, Snow and Soil moisture Model
Intercomparison Program – aims, set-up and expected outcome**

Bart van den Hurk¹, Hyungjun Kim², Gerhard Krinner³, Sonia I. Seneviratne⁴, Chris Derksen⁵,
Taikan Oki², Hervé Douville⁶, Jeanne Colin⁶, Agnès Ducharne⁷, Frederique Cheruy⁷, Nicholas
Viovy⁸, Michael Puma⁹, Yoshihide Wada¹⁰, Weiping Li¹¹, Binghao Jia¹², Andrea Alessandri¹³,
Dave Lawrence¹⁴, Graham P. Weedon¹⁵, Richard Ellis¹⁶, Stefan Hagemann¹⁷, Jiafu Mao¹⁸,
Mark G Flanner¹⁹, Matteo Zampieri²⁰, Rachel Law²¹, and Justin Sheffield^{22,23}

¹ *KNMI The Netherlands (corresponding author: hurkvd@knmi.nl)*

² *Univ Tokyo Japan – MIROC6*

³ *LGGE Grenoble France – IPSL*

⁴ *ETH Zürich Switzerland*

⁵ *Environment and climate change Canada – CCCma*

⁶ *CNRM France – CNRM*

⁷ *UPMC France – IPSL*

⁸ *LSCE France – IPSL*

⁹ *NASA US – GISS*

¹⁰ *IIASA Laxenburg Austria*

¹¹ *CMA China – BCC*

¹² *Chinese Academy of Sciences – FGOALS*

¹³ *ENEA Italy – EC-Earth*

¹⁴ *NCAR Boulder – CESM*

¹⁵ *UK Metoffice*

¹⁶ *CEH Wallingword – hadGEM3*

¹⁷ *Max Planck Hamburg – MPI*

¹⁸ *Oak Ridge National Laboratory – ACME Land model*

¹⁹ *University of Michigan USA*

²⁰ *CMCC and University of Bologna – CMCC-CM2*

²¹ *CSIRO Australia – ACCESS*

²² *Princeton University USA*

²³ *University of Southampton, UK*

33

34

Revised Manuscript submitted to GMD

35

36

v1, 13 July 2016

37

38

Abstract

The Land Surface, Snow and Soil Moisture Model Intercomparison Project (LS3MIP) is designed to provide a comprehensive assessment of land surface, snow, and soil moisture feedbacks on climate variability and climate change, and to diagnose systematic biases in the land modules of current Earth System Models (ESMs). The solid and liquid water stored at the land surface has a large influence on the regional climate, its variability and predictability, including effects on the energy, water and carbon cycles. Notably, snow and soil moisture affect surface radiation and flux partitioning properties, moisture storage and land surface memory. They both strongly affect atmospheric conditions, in particular surface air temperature and precipitation, but also large-scale circulation patterns. However, models show divergent responses and representations of these feedbacks as well as systematic biases in the underlying processes. LS3MIP will provide the means to quantify the associated uncertainties and better constrain climate change projections, which is of particular interest for highly vulnerable regions (densely populated areas, agricultural regions, the Arctic, semi-arid and other sensitive terrestrial ecosystems).

The experiments are subdivided in two components, the first addressing systematic land biases in offline mode (“LMIP”, building upon the 3rd phase of Global Soil Wetness Project; GSWP3) and the second addressing land feedbacks attributed to soil moisture and snow in an integrated framework (“LFMIP”, building upon the GLACE-CMIP blueprint).

Introduction

Land surface processes, including heat fluxes, snow, soil moisture, vegetation, turbulent transfer and runoff, continue to be ranked highly on the list of the most relevant yet complex and poorly represented features in state-of-the-art climate models. People live on land, exploit its water and natural resources, and experience day-to-day weather that is strongly affected by feedbacks with the land surface. The six Grand Challenges of the World Climate Research Program (WCRP)¹ include topics governed primarily (Water Availability, Cryosphere) or largely (Climate Extremes) by land surface characteristics.

Despite the importance of a credible representation of land surface processes in Earth System Models (ESMs), a number of systematic biases and uncertainties persist. Biases in hydrological characteristics (e.g. moisture storage in soil and snow, runoff, vegetation and surface water bodies), partitioning of energy and water fluxes (Seneviratne et al. 2010), definition of initial and boundary conditions at the appropriate spatial scale, feedback strengths (Koster et al. 2004; Qu and Hall 2014) and inherent land surface related predictability (Douvillie et al. 2007; Dirmeyer et al. 2013) are still subjects of considerable research effort.

These biases and uncertainties are problematic, because they affect, among others, forecast skill (Koster et al. 2010a), regional climate change patterns (Campoy et al. 2013; Seneviratne

¹ <http://www.wcrp-climate.org/grand-challenges>

et al. 2013; Koven et al. 2012), and explicable trends in water resources (Lehning 2013). In addition, there is evidence of the presence of large-scale systematic biases in some aspects of land hydrology in current climate models (Mueller and Seneviratne 2014) and the terrestrial component of the carbon cycle (Anav et al. 2013; Mystakidis et al. 2016). Notably, land surface processes can be an important reason for a direct link between the climate models' temperature biases in the present period and in the future projections with increased radiative forcings at the regional scale (Cattiaux et al. 2013).

For snow cover, a better understanding of the links with climate is critical for interpretation of the observed dramatic reduction in springtime snow cover over recent decades (e.g. (Derksen and Brown 2012; Brutel-Vuilmet et al. 2013), to improve the seasonal to interannual forecast skill of temperature, runoff and soil moisture (e.g. Thomas et al. 2015; Peings et al. 2011), and to adequately represent polar warming amplification in the Arctic (e.g. Holland and Bitz, 2003). Snow-related biases in climate models may arise from the snow-albedo feedback (Qu and Hall 2014; Thackeray et al. 2015a), but also from the energy sink induced by snow melting in spring and the thermal insulation effect of snow on the underlying soil (Koven et al. 2012; Gouttevin et al. 2012). Temporal dynamics of snow-atmospheric coupling during various phases of snow depletion (Xu and Dirmeyer 2011, 2012) are crucial for a proper representation of the timing and atmospheric response to snow melt. Phase 1 and 2 of the Snow Model Intercomparison Project (SnowMIP) (Etchevers et al. 2004; Essery et al. 2009) provided useful insights in the capacity of snow models of different complexity to simulate the snowpack evolution from local meteorological forcing but did not explore snow-climate interactions. Because of strong snow/atmosphere interactions, it remains difficult to distinguish and quantify the various potential causes for disagreement between observed and modeled snow trends and the related climate feedbacks.

Soil moisture plays a central role in the coupled land – vegetation – snow – water – atmosphere system (Seneviratne et al., 2010; van den Hurk et al., 2011), where interactions are evident at many relevant time scales: diurnal cycles of land surface fluxes, seasonal and subseasonal predictability of droughts, floods, and hot extremes, annual cycles governing the water buffer in dry seasons, and shifts in the climatology in response to changing patterns of precipitation and evaporation. The representation of historical variations in land water availability and droughts still suffer from large uncertainties, due to model parameterizations, unrepresented hydrologic processes such as lateral groundwater flow, lateral flows connected to reinfiltration of river water or irrigation with river water, and/or atmospheric forcings (Sheffield et al. 2012; Zampieri et al. 2012; Trenberth et al. 2014; Greve et al. 2014; Clark et al. 2015). This also applies to the energy and carbon exchanges between the land and the atmosphere (e.g. Mueller and Seneviratne 2014; Friedlingstein et al. 2013).

It is difficult to generate reliable observations of soil moisture and land surface fluxes that can be used as boundary conditions for modelling and predictability studies. Satellite retrievals, in situ observations, offline model experiments (Second Global Soil Wetness Project, GSWP2; Dirmeyer et al. 2006) and indirect estimates all have a potential to

generate relevant information but are largely inconsistent, covering different model components, and suffer from methodological flaws (Mueller et al. 2013; Jiafu Mao et al. 2015). As a consequence, the pioneering work on deriving soil moisture related land-atmosphere coupling strength (Koster et al. 2004) and regional/global climate responses in both present and future climate (Seneviratne et al. 2006, 2013) has been carried out using (ensembles of) modelling experiments. The second Global Land Atmosphere Coupling Experiment (GLACE2; Koster et al., 2010a) measured the actual temperature and precipitation skill improvement of using GSWP2 soil moisture initializations, which is much lower than suggested by the coupling strength diagnostics. Limited quality of the initial states, limited predictability and poor representation of essential processes determining the propagation of information through the hydrological cycle in the models all play a role.

Altogether, there are substantial challenges concerning both the representation of land-surface processes in current-generation ESMs and the understanding of related climate feedbacks. The Land Surface, Snow and Soil moisture Model Intercomparison Project (LS3MIP) is designed to allow the climate modelling community to make substantial progress in addressing these challenges. It is part of the sixth phase of the Coupled Model Intercomparison Project (CMIP6; Eyring et al. 2015). The following section further develops the objectives and rationale of LS3MIP. The experimental design and analysis plan is presented thereafter. The final discussion section describes the expected outcome and impact of LS3MIP.

Objectives and rationale

The goal of the collection of LS3MIP experiments is to provide a comprehensive assessment of land surface, snow, and soil moisture-climate feedbacks, and to diagnose systematic biases and process-level deficiencies in the land modules of current ESMs. While vegetation, carbon cycle, soil moisture, snow, surface energy balance and land-atmosphere interaction are all intimately coupled in the real world, LS3MIP focuses – necessarily – on the physical land surface in this complex system: interactions with vegetation and carbon cycle are included in the analyses wherever possible without losing this essential focus. In the complementary experiment Land Use MIP (LUMIP; see Lawrence et al. submitted) and C4MIP (Jones et al. 2016) vegetation, the terrestrial carbon cycle and land management are the central topics of analysis. LS3MIP and LUMIP share some model experiments and analyses (see below) to allow to be addressed the complex interactions at the land surface and yet remain able to focus on well-posed hypotheses and research approaches.

LS3MIP will provide the means to quantify the associated uncertainties and better constrain climate change projections, of particular interest for highly vulnerable regions (including densely populated regions, the Arctic, agricultural areas, and some terrestrial ecosystems).

The LS3MIP experiments collectively address the following objectives:

- evaluate the current state of land processes including surface fluxes, snow cover and soil moisture representation in CMIP DECK (Diagnostic, Evaluation and Characterization of

Klima) experiments and CMIP6 historical simulations (Eyring et al. 2015), to identify the main systematic biases and their dependencies;

- estimate multi-model long-term terrestrial energy/water/carbon cycles, using the land modules of CMIP6 models under observation-constrained historical (land reanalysis) and projected future (impact assessment) climatic conditions considering land use/land cover changes;

- assess the role of snow and soil moisture feedbacks in the regional response to altered climate forcings, focusing on controls of climate extremes, water availability and high-latitude climate in historical and future scenario runs;

- assess the contribution of land surface processes to systematic Earth System model biases and the current and future predictability of regional temperature/precipitation patterns.

These objectives address each of the three CMIP6 overarching questions: 1) What are regional feedbacks and responses to climate change?; 2) What are the systematic biases in the current climate models?; and 3) What are the perspectives concerning the generation of predictions and scenarios?

LS3MIP encompasses a family of model experiments building on earlier multi-model experiments, particularly a) offline land surface experiments (GSWP2 and its successor GSWP3), b) the coordinated snow model intercomparisons SnowMIP phase 1 and 2 (Etchevers et al., 2002; Essery et al., 2009), and c) the coupled climate time-scale GLACE-type configuration (GLACE-CMIP, Seneviratne et al. 2013). Within LS3MIP the Land-only experimental suite is referred to as **LMIP (Land Model Intercomparison Project)** with the experiment ID **Land**, while the coupled suite is labelled as **LFMIP (Land Feedback MIP)**. A detailed description of the model design is given below, and a graphical display of the various components within LS3MIP is shown in Figure 1.

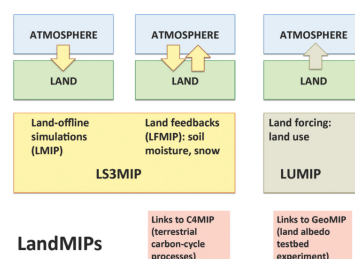
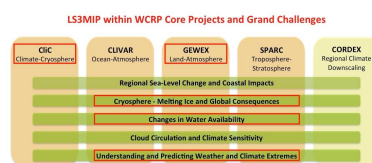


Figure 1: Structure of the “LandMIPs”. LS3MIP includes (1) the offline representation of land processes (LMIP) and (2) the representation of land-atmosphere feedbacks related to snow and soil moisture (LFMIP). Forcing associated with land use is assessed in LUMIP. Substantial links also exist to C4MIP (terrestrial carbon cycle). Furthermore, a land albedo testbed experiment is planned within GeoMIP. From Seneviratne et al. (2014)

192



193

194 *Figure 2: Relevance of LS3MIP for WCRP Core Projects and Grand Challenges²*

195

196 As illustrated in Figure 2, LS3MIP is addressing multiple WCRP Grand Challenges and core
 197 projects. The LMIP experiment will provide better estimates of historical changes in snow
 198 and soil moisture at global scale, thus allowing the evaluation of changes in freshwater,
 199 agricultural drought, and streamflow extremes over continents, and a better understanding
 200 of the main drivers of these changes. The LFMIP experiments are of high relevance for the
 201 assessment of key feedbacks and systematic biases of land surfaces processes in coupled
 202 mode (Dirmeyer et al. 2015), and are particularly focusing on two of the main feedback
 203 loops over land: the snow-albedo-temperature feedback involved in Arctic Amplification,
 204 and the soil moisture-temperature feedback leading to major changes in temperature
 205 extremes (Douville et al. 2016). In addition, LS3MIP will allow the exchange of data and
 206 knowledge across the snow and soil moisture research communities that address a common
 207 physical topic: terrestrial water in liquid and solid form. Snow and soil moisture dynamics
 208 are often interrelated (e.g. Hall et al. 2008; Xu and Dirmeyer 2012) and jointly contribute to
 209 hydrological variability (e.g. Koster et al. 2010b).

210 LS3MIP will also provide relevant insights for other research communities, such as global
 211 reconstructions of land variables that are not directly observed for detection and attribution
 212 studies (Douville et al. 2013), estimates of freshwater inputs to the oceans (which are
 213 relevant for sea-level changes and regional impacts; Carmack et al. 2015), the assessment of
 214 feedbacks shown to strongly modulate regional climate variability relevant for regional
 215 climate information, as well as the investigation of land climate feedbacks on large-scale
 216 circulation patterns and cloud occurrence (Zampieri and Lionello 2011). This will thus also
 217 imply potential contributions to programmes like the Inter-Sectoral Impact Model
 218 Intercomparison Project (ISIMIP; Warszawski et al. 2014) and the International Detection
 219 and Attribution Group IDAG. LS3MIP is geared to extend and consolidate available data,
 220 models and theories to support human awareness and resilience to highly variable
 221 environmental conditions in a large ensemble of sectoral domains, including disaster risk
 222 reduction, food security, public safety, nature conservation and societal wellbeing.

223

² <http://wcrp-climate.org/index.php/grand-challenges>; status Dec 2015

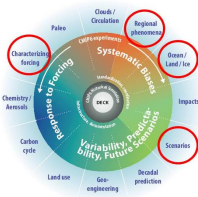


Figure 3: Embedding of LS3MIP within CMIP6. Adapted from Eyring et al. (2015)

Figure 3 illustrates the embedding of LS3MIP within CMIP6. LS3MIP fills a major gap by considering systematic land biases and land feedbacks. In this context, LS3MIP is part of a larger “LandMIP” series of CMIP6 experiments fully addressing biases, uncertainties, feedbacks and forcings from the land surface (Figure 1), which are complementary to similar experiments for ocean or atmospheric processes (Seneviratne et al. 2014). In particular, we note that while LS3MIP focuses on systematic biases in land surface processes (Land) and on feedbacks from the land surface processes on the climate system (LFMIP), the complementary Land Use MIP (LUMIP) experiment addresses the role of land use forcing on the climate system. The role of vegetation and carbon stores in the climate system is a point of convergence between LUMIP, C4MIP and LS3MIP, and the offline LMIP experiment will serve as land-only reference experiments for both the LS3MIP and LUMIP experiments. In addition, there will also be links to the C4MIP experiment with respect to impacts of snow and soil moisture processes (in particular droughts and floods) on terrestrial carbon exchanges and resulting feedbacks to the climate system.

Experimental design

The experimental design of LS3MIP consists of a series of offline land-only experiments (LMIP) driven by a land surface forcing data set and a variety of coupled model simulations (LFMIP) (see Figure 4 and Table 1):

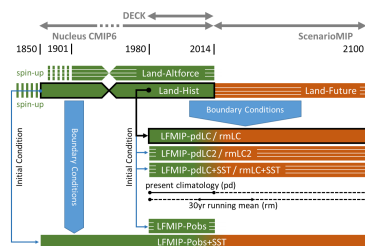


Figure 4: Schematic diagram for the experiment structure of LS3MIP. Tier 1 experiments are indicated with a heavy black outline, and complementary ensemble experiments are indicated with white hatched lines. Land-Altforc represents 3 alternative forcings for the Land-Hist experiment. For further details on the experiments and acronyms, see Table 1 and text.

(1) Offline land model experiments (“Land offline MIP”, experiment ID “Land”):

Offline simulations of land surface states and fluxes allow for the evaluation of trends and variability of snow, soil moisture and land surface fluxes, carbon stocks and vegetation dynamics, and climate change impacts. Within the CMIP6 program various Model Intercomparison Projects make use of offline terrestrial simulations to benchmark or force coupled climate model simulations: LUMIP focusing on the role of land use/land cover change, C4MIP to address the terrestrial component of the carbon cycle and its feedback to climate, and LS3MIP to provide soil moisture and snow boundary conditions.

Meteorological forcings, ancillary data (e.g., land use/cover changes, surface parameters, CO₂ concentration and nitrogen deposition) and documented protocols to spin-up and execute the experiments are essential ingredients for a successful offline land model experiment (Wei et al. 2014). The first Global Soil Wetness Project (GSWP; Dirmeyer et al. 1999), covering two annual cycles (1987 – 1988), established a successful template, which was updated and fine-tuned in a number of follow-up experiments, both with global (Dirmeyer et al. 2006; Sheffield et al. 2006) and regional (Boone et al. 2009) coverage.

Available data sets for meteorological forcing

Offline experiments will primarily use GSWP3³ (Tier 1) forcing (Kim et al., in preparation) with alternate forcing used in Tier 2 experiments.

The third Global Soil Wetness Project (GSWP3) provides meteorological forcings for the entire 20th century and beyond, making extensive use of the 20th Century Reanalysis (20CR) (Compo et al. 2011). In this reanalysis product only surface pressure and monthly sea-surface temperature and sea-ice concentration are assimilated. The ensemble uncertainty in the synoptic variability of 20CR varies with the time-changing observation network. High correlations for geopotential height (500 hPa) and air temperature (850 hPa) with an independent long record (1905-2006) of upper-air data were found (Compo et al. 2011), comparable to forecast skill of a state-of-the-art forecasting system at 3 days lead time.

GSWP3 forcing data are generated based on a dynamical downscaling of 20CR. A simulation of the Global Spectral Model (GSM), run at a T248 resolution (~50km) is nudged to the vertical structures of 20CR zonal and meridional winds and air temperature using a spectral nudging dynamical downscaling technique that effectively retains synoptic features in the higher spatial resolution (Yoshimura and Kanamitsu 2008). Additional bias corrections using observations, vertical damping (Hong and Chang 2012) and single ensemble member correction (Yoshimura and Kanamitsu 2013) are applied, giving considerable improvements.

Weedon et al. (2011) provide the meteorological forcing data for the EU Water and Global Change (WATCH) programme⁴, designed to evaluate global hydrological trends and impacts using offline modelling. The half-degree resolution, 3 hourly WATCH Forcing Data (WFD) was based on the ECMWF ERA-40 reanalysis and included elevation correction and monthly bias correction using CRU observations (and alternative GPCC precipitation total

³ <http://hydro.iis.u-tokyo.ac.jp/GSWP3/>

⁴ <http://www.eu-watch.org/>

observations). WATCH hydrological modelling led to the WaterMIP study (Haddeland et al. 2011). The WFD stops in 2001, but within a follow-up project EMBRACE Weedon et al. (2014) generated the WFDEI dataset that starts in 1979 and was recently extended to 2014. The WFDEI was based on the WATCH Forcing Data methodology but used the ERA-Interim reanalysis (4D-var and higher spatial resolution than ERA-40) so that there are offsets for some variable in the overlap period with the WFD. The forcing consists of 3-hourly ECMWF ERA-Interim reanalysis data (WFD used ERA-40) interpolated to half degree spatial resolution. The 2m temperatures are bias-corrected in terms of monthly means and monthly average diurnal temperature range using CRU half degree observations. The 2m temperature, surface pressure, specific humidity and downwards long-wave radiation fluxes are sequentially elevation corrected. Short-wave radiation fluxes are corrected using CRU cloud cover observations and corrected for the effects of seasonal and interannual changes in aerosol loading. Rainfall and snowfall rates are corrected using CRU wet days per month and according to CRU or GPCC observed monthly precipitation gauge totals. The WFDEI data set is also used as forcing to the ISIMIP2.1 project, which focuses on historical validation of global water balance under transient land use change (Warszawski et al. 2014).

To support the Global Carbon Project⁵ (Le Quere et al. 2009) with annual updates of global carbon pools and fluxes, the offline modelling framework TRENDY⁶ applies an ensemble of terrestrial carbon allocation and land surface models. For this a forcing data set is prepared in which NCEP reanalysis data are bias corrected using the gridded in situ climate data from the Climate Research Unit (CRU), the so-called CRU-NCEP dataset⁷. This dataset is currently available from 1901 to 2014 at 0.5 degrees horizontal spatial resolution and 6 hourly time-step. It is being updated annually.

The Princeton Global Forcing dataset⁸ (Sheffield et al. 2006) was developed as a forcing for land surface and other terrestrial models, and for analyzing changes in near surface climate. The dataset is based on 6-hourly surface climate from the NCEP-NCAR reanalysis, which is corrected for biases at diurnal, daily and monthly time scales using a variety of observational datasets. The data are available at 1.0, 0.5 and 0.25-degree resolution and 3-hourly time-step. The latest version (V2.2) covers 1901-2014, with a real-time extension based on satellite precipitation and weather model analysis fields. The reanalysis precipitation is corrected by adjusting the number of rain days and monthly accumulations to match observations from CRU and the Global Precipitation Climatology Project (GPCP). Precipitation is downscaled in space using statistical relationships based on GPCP and the TRMM Multi-satellite Precipitation Analysis (TMPA), and to 3-hourly resolution based on TMPA. Temperature, humidity, pressure and longwave radiation are downscaled in space with account for elevation. Daily mean temperature and diurnal temperature range are

⁵ <http://www.globalcarbonproject.org/about/index.htm>

⁶ <http://dgvm.ceh.ac.uk/node/21>

⁷ Viovy N, Ciais P (2009) A combined dataset for ecosystem modelling, Available at: <http://dods.extra.cea.fr/data/p529viov/cruncep/readme.htm>

⁸ <http://hydrology.princeton.edu/data.php>

adjusted to match the CRU monthly data. Short- and long-wave surface radiation are adjusted to match satellite-based observations from the University of Maryland (Zhang et al. submitted) and to be consistent with CRU cloud cover observations outside of the satellite period. An experimental version (V3) assimilates station observations into the background gridded field to provide local-scale corrections (Sheffield et al., in preparation).

Figure 5 shows the performance in terms of correlation and standard deviation of the forcing data sets compared to daily observations from 20 globally distributed in-situ FLUXNET sites (Baldocchi et al. 2001). Although for precipitation intrinsic heterogeneity leads to significant differences with the in-situ observations, long- and short-wave downward radiation (not shown) and air temperature show variability characteristics similar to the observations.

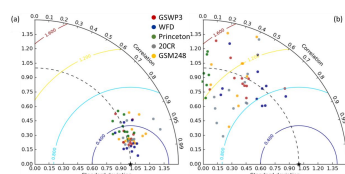


Figure 5: Taylor diagram for evaluating the forcing datasets comparing to daily observations from FLUXNET sites, as used by Best et al. (2015): (a) 2m air temperature and (b) precipitation. Red, blue, and green dots indicate GSWP3, Watch Forcing Data (Weedon et al. 2011) and Princeton forcing (Sheffield et al. 2006), respectively. Grey and orange dots indicate 20CR and its dynamically downscaled product (GSM248).

The participating modelling groups are invited to run a number of experiments in this land-only branch of LS3MIP.

Historical offline simulations: Land-Hist

The Tier 1 experiments of the offline LMIP experiment consist of simulations using the GSWP3 forcing data for a historical (1831-2014) interval. The land model configuration should be identical to that used in the DECK and CMIP6 historical simulations for the parent coupled model.

The atmospheric forcing will be prepared at a standard $0.5 \times 0.5^\circ$ spatial resolution at 3 hourly intervals and distributed with a package to regrid data to the native grids of the GCMs. Also vegetation, soil, topography and land/sea mask data will be prescribed following the protocol used for the CMIP6 DECK simulations. Spin-up of the land-only simulations should follow the TRENDY protocol⁹ which calls for recycling of the climate mean and variability from two decades of the forcing dataset (e.g., 1831-1850 for GSWP3, 1901-1920 for the alternative land surface forcings). Land use should be held constant at 1850 as in the DECK 1850 coupled control simulation (*piControl*). See discussion and definition of “constant land-use” in Section 2.1 of LUMIP protocol paper (Lawrence et al. submitted). CO₂ and all other forcings should be held constant at 1850 levels during spinup.

⁹ <http://dgvm.ceh.ac.uk/node/9>

For the period 1850 to the first year of the forcing dataset, the forcing data should continue to be recycled but all other forcings (land-use, CO₂, etc.) should be as in the CMIP6 historical simulation. Transient land use is a prescribed CMIP6 forcing and is described in the LUMIP protocol (Lawrence et al. submitted).

Interactions with the Ocean MIP (OMIP; Griffies et al. 2016) are arranged by the use of terrestrial freshwater fluxes produced in the LMIP simulations as a boundary condition for the forced ocean-only simulations in OMIP, in addition to the forcing provided by (Dai and Trenberth 2002).

Single site time series of in-situ observational forcing variables from selected reference locations (from FLUXNET, Baldocchi et al. 2001) are supplied in addition to the forcing data for additional site level validation.

Although Land-Hist is not a formal component of the DECK simulations which form the core of CMIP6 (see Figure 3), the WCRP Working Group on Climate Modelling (WGCM) recognized the importance of these land-only experiments for the process of model development and benchmarking. A future implementation of a full or subset of this historical run is proposed to become part of the DECK in future CMIP exercises and is included as a Tier 1 experiment in LS3MIP. Land surface model output from this subset of LMIP will also be used as boundary condition in some of the coupled climate model simulations, described below.

Historical simulations with alternative forcings

Additional Tier 2 experiments are solicited where the experimental set-up is similar to the Tier 1 simulations, but using 3 alternative meteorological forcing data sets that differ from GSWP3: the Princeton forcing (Sheffield et al. 2006), WFD and WFDEI combined (allowing for offsets as needed (Weedon et al. 2014) and the CRU-NCEP forcing (Wei et al. 2014) used in TRENDY (Sitch et al. 2015). These Tier 2 experiments cover the period 1901 – 2014. The model outputs will allow assessment of the sensitivity of land-only simulations to uncertainties in forcing data. Differences in the outputs compared to the primary runs with the GSWP3 forcing will help in understanding simulation sensitivity to the selection of forcing datasets. Kim (2010) utilized a similarity index (Ω ; Koster et al. 2000) to estimate the uncertainty derived from an ensemble of precipitation observation data sets relative to the the uncertainty from an ensemble of model simulations for evapotranspiration and runoff. The joint utilization of common monthly observations by the various forcing data sets leads to a high value of Ω when evaluated using monthly mean values. However, evaluation of dataset consistency of monthly variance leads to much larger disparities and considerably lower values of Ω (Figure 6). This uncertainty will propagate differently to other hydrological variables, such as runoff or evapotranspiration (Kim 2010).

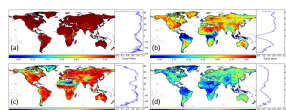


Figure 6: Global distributions of the similarity index (Ω) for 2001-2010 of monthly mean (a, c) and (b, d) monthly variance (calculated from daily data from each data set) of 2m air temperature (top panels) and precipitation (bottom panels), respectively. Shown are global distributions and zonal means. After (Kim 2010).

Climate change impact assessment: Land-Future

A set of future land-only time slice simulations (2015-2100) will be generated via forcing data obtained from at least 2 future climate scenarios from the ScenarioMIP (O'Neill et al. 2016) and will be executed at a later stage during CMIP6. Tentatively, Shared Socio-economic Pathway SSP5-8.5 and SSP4-3.7¹⁰ will be selected, run by 3 model realizations each. The models will be chosen based on the evaluation of the results from the Historical simulations from the CMIP6 Nucleus in order to represent the ensemble spread efficiently and reliably (Evans et al. 2013). To generate a set of ensemble forcing data for the future, a trend preserving statistical bias correction method will be applied to the 3-hourly surface meteorology variables (Table A4) from the scenario output (Hempel et al. 2013; Watanabe et al. 2014). Gridded forcings will be provided in a similar data format as the historical simulations.

Land-Future is a Tier 2 experiment in LS3MIP and focuses on assessment of climate change impact (e.g. shifts of the occurrence of critical water availability due to changing statistical distributions of extreme events) and on the assessment of the land surface analogue of climate sensitivity for various key land variables (Perket et al. 2014; Flanner et al. 2011).

(2) Prescribed land surface states in coupled models for land surface feedback assessment ("Land Feedback MIP", LFMIP):

Land surface processes do not act in isolation in the climate system. A tight coupling with the overlying atmosphere takes place on multiple temporal and spatial scales. A systematic assessment of the strength and spatial structure of land surface interaction at subcontinental, seasonal time scales has been performed with the initial GLACE set-up (GLACE1 and GLACE2 experiments; Koster et al. (2004)) in which essentially the spread in an ensemble simulation of a coupled land-atmosphere model was compared to a model configuration in which the land-atmosphere interaction was greatly bypassed by prescribing soil conditions throughout the simulation in all members of the ensemble. Examination of the significance of land-atmosphere feedbacks at the centennial climate time scale was later explored at the regional scale in a single-model study (Seneviratne et al. 2006) and on global scale in the GLACE-CMIP5 experiment in a small model ensemble (Seneviratne et al. 2013).

A protocol very similar to the design of GLACE-CMIP5 is followed in LFMIP. Parallel to a set of reference simulations taken from the CMIP6 DECK, a set of forced experiments is carried out where land surface states are prescribed from or nudged towards prescribed fields derived from coupled simulations. The land surface states are prescribed or nudged at a

¹⁰ <https://cmip.ucar.edu/scenario-mip/experimental-protocols>

daily time scale. This set-up is similar to the Flux Anomaly Forced MIP (FAFMIP, Gregory et al. 2016), where the role of ocean-atmosphere interaction at climate time scales is diagnosed by idealised surface perturbation experiments.

While earlier experiments used model configurations with prescribed SST and sea ice conditions, the Tier 1 experiment in LFMIP will be based on coupled AOGCM simulations and comprise simulations for a historical (1980-2014) and future (2015-2100) time range. The selection of the future scenario (from the ScenarioMIP experiment) will be based on the choices made in the offline LMIP experiment (see above).

In GLACE-CMIP5 only soil moisture states were prescribed in the forced experiments. The configuration of the particular land surface models may introduce the need to make different selections of land surface states to be prescribed, for instance to avoid strong inconsistencies in the case of frozen ground (soil moisture rather than soil water state should be prescribed; *M. Hauser, ETH Zurich, personal communication*), melting snow, or growing vegetation. Prescribing surface soil moisture only (experiment “S” in Koster et al. 2006) gave unrealistic values of the surface Bowen ratio. A standardization of this selection is difficult as the implementation and consequences may be highly model specific. Here we recommend to prescribe only the water reservoirs (soil moisture, snow mass). The disparity of possible implementations is adding to the uncertainty range generated by the model ensemble, similar to the degree to which implementation of land use, flux corrections or downscaling adds to this uncertainty range. Participating modelling groups are encouraged to apply various test simulations focusing both on technical feasibility and experimental impact to evaluate different procedures to prescribe land surface conditions.

The earlier experience with GLACE-type experiments has revealed a number of technical and scientific issues. Because in most GCMs the land surface module is an integral part of the code describing the atmosphere, prescribing land surface dynamics requires a non-conventional technical interface, reading and replacing variables throughout the entire simulations. Many LS3MIP participants have participated earlier in GLACE-type experiments, but for some the code adjustments will require a technical effort. Interpretation of the effect of the variety of implementations of prescribed land surface variables by the different modelling groups (see above) is helped by a careful documentation of the way the modelling groups have implemented this interface. Tight coordination and frequent exchange among the participating modelling groups on the technical modalities of the implementation of the required forcing methods will be ensured during the preparatory phase of LS3MIP in order to maximize the coherence of the modelling exercise and to facilitate the interpretation of the results.

By design, the prescribed land surface experiments do not fully conserve water and energy, similar to AMIP, nudged, and data assimilation experiments. A systematic addition or removal of water or energy can even emerge as a result of asymmetric land surface responses to dry and to wet conditions, e.g. when surface evaporation or runoff depend strongly non-linearly to soil moisture or snow states (e.g. Jaeger and Seneviratne 2011). Also, unrepresented processes (such as water extraction for irrigation or exchange with the groundwater) may lead to imbalances in the budget (Wada et al. 2012). This systematic

alteration of the water and energy balance may not only perturb the simulation of present-day climate (e.g. Douville 2003; Douville et al. 2016) but may also interact with the projected climate change signal, where altered climatological soil conditions can contribute to the climate change induced temperature or precipitation signal or water imbalances can lead to imposed runoff changes that could affect ocean circulation and SSTs. Earlier GLACE-type experiments revealed that the problems of water conversion are often reduced when prescribed soil water conditions are taken as the median rather than the mean of a sample over which a climatological mean is calculated (Hauser et al. *subm*). In the analyses of the experiments this asymmetry and lack of energy/water balance closure will be examined and put in context of the climatological energy and water balance and its climatic trends.

To be able to best quantify the forcing that prescribing the land surface state represents, the increments of both snow and soil moisture imposed as a consequence of this prescription are required as an additional output. This will enable us to estimate the amplitude of implicit water and energy fluxes imposed by the forcing procedure.

Complementary experiments following an almost identical setup as LFMIP, but limiting the prescription of land surface variables to snow-related variables and thus leaving soil moisture free-running, are carried out in the framework of the ESM-SnowMIP (Earth System Model - Snow Module Intercomparison Project) carried out within the WCRP Grand Challenge “Melting Ice and Global Consequences”¹¹. ESM-SnowMIP being tightly linked to LS3MIP, these complementary experiments will allow separating effects of soil moisture and snow feedbacks.

Tier 1 experiments in LFMIP

Similar to the set-up of GLACE-CMIP5 (Seneviratne et al. 2013), the core experiments of LFMIP (tier 1) evaluate two different sets of prescribed land surface conditions (snow and soil moisture):

- LFMIP-pdLC: the experiments comprise transient coupled atmosphere-ocean simulations in which a selection of land surface characteristics is prescribed rather than interactively calculated in the model. This “climatological” land surface forcing is calculated as the mean annual cycle in the period 1980-2014 from the Historical GCM simulations. The experiment aims at diagnosing the role of land-atmosphere feedback at the climate time scale. Seneviratne et al. (2013) found a substantial effect of changes in climatological soil moisture on projected temperature change in a future climate, both for seasonal mean and daytime extreme temperature in summer. Effects on precipitation are less clear, and the multi-model nature of LS3MIP is designed to sharpen these quantitative effects. Also, LS3MIP will take a potential damping (or amplifying) effect of oceanic responses on altered land surface conditions into account, in contrast to GLACE-CMIP5. Experiments using this set-up (i.e. coupled ocean) in a single-model study have shown that the results could be

¹¹ <http://www.climate-cryosphere.org/activities/targeted/esm-snowmip>

slightly affected by the inclusion of an interactive ocean, although the effects were not found to be large overall (Orth and Seneviratne submitted).

- LFMIP-rmLC: a prescribed climatology using a transient 30-yr running mean, where a comparison to the standard CMIP6 runs allows diagnosis of shifts in the regions of strong land-atmosphere coupling as recorded by e.g. Seneviratne et al. (2006), and shifts in potential predictability related to land surface states (Dirmeyer et al. 2013).

Both sets of simulations cover the historical period (1850-2014) and extend to 2100, based on a forcing scenario to be identified at a later stage. The procedure to initialize the land surface states in the ensemble members is left to the participant, but should allow to generate sufficient spread that can be considered representative for the climate system under study. Koster et al. (2006) proposed a preference hierarchy of methods depending on the availability of initialization fields, and LS3MIP will follow this proposal.

Output in high temporal resolution (daily, as well as sub-daily for some fields and time slices) is required to address the role of land surface-climate feedbacks on climate extremes over land.

Multi-member experiments are encouraged, but the mandatory tier 1 simulations are limited to one realization for each of the two prescribed land surface time series described above.

Tier 2 experiments in LFMIP

To analyse a number of additional features of land –atmosphere feedbacks, a collection of tier 2 simulations is proposed in LS3MIP:

- *Simulations with observed SST:* The AOGCM simulations from Tier 1 are duplicated with a prescribed SST configuration taken from the AMIP runs in the DECK (AGCM), in order to isolate the role of the ocean in propagating and damping/reinforcing land surface responses on climate (Koster et al. 2000). Both the historic and running mean land surface simulations are requested (LFMIP-pdLC+SST and –rmLC+SST, respectively)
- *Simulations with observed SST and Land-hist output:* A “pseudo-observed boundary condition” set of experiments use the AMIP SSTs and the Land-Hist land boundary conditions generated by the land surface model used in the participating ESM, leading to simulations driven by surface fields that are strongly controlled by observed forcings. This will only cover the historic period (1901-2014) (LFMIP-PObs+SST). For this the land-only simulations in LMIP need to be interpolated to the native GCM grid, preserving land-sea boundaries and other characteristics.
- *Separate effects of soil moisture and snow, and role of additional land parameters and variables:* Additional experiments, in which only snow, snow albedo or soil moisture is prescribed will be conducted to assess the respective feedbacks in isolation, and have control on possible interactions between snow cover and soil moisture content. Also vegetation parameters and variables (e.g. leaf area index,

canopy height and thickness) are considered. These experiments are not listed in Table 1, but will be detailed in a follow-up protocol to be defined later.

- *Fixed land use conditions:* in conjunction with the Land Use MIP (LUMIP) a repetition of the Tier 1 experiment under fixed 1850 land cover and land use conditions highlights the role of soil moisture in modulating the climate response to land cover and land use (Not listed in Table 1).

(3) Prescribed land surface states derived from pseudo-observations (LFMIP-Pobs)

The use of LMIP (land-only simulations) to initialize the AOGCM experiments (LFMIP) allows a set of predictability experiments in line with the GLACE2 set-up (Koster et al. 2010a). The LFMIP-Pobs experiment is an extension to GLACE2 by (a) allowing more models to participate, (b) improving the statistics by extending the original 1986 – 1995 record to 1980 – 2014, (c) evaluating the quality of newly available land surface forcings, and (d) executing the experiments in AOGCM mode. Koster et al. (2010a) and van den Hurk et al. (2012) concluded that the forecast skill improvement from models using initial soil moisture conditions was relatively low. Possible causes for this low skill are the limited record length and limited quality of the (precipitation) observations used to generate the soil conditions. These issues are explicitly addressed in LFMIP-Pobs.

All LFMIP-Pobs experiments are Tier 2, which also gives room for additional model design elements such as the evaluation of various observational data sources (such as for SWE or snow albedo, using satellites derived, reanalysis and land surface model outputs). The predictability assessments include the evaluation of the contribution of snow cover melting and its related feedbacks to the underestimation of recent boreal polar warming by climate models.

The experimental protocol (number of simulations years, ensemble size, initialization, model configuration, output diagnostics) has a strong impact on the results of the experiment (e.g. Guo and Dirmeyer 2013). This careful design of the LFMIP-Pobs experiment needed for a successful implementation has currently not yet taken place. Therefore these experiments are listed as Tier 2 in Table 1, with the comment that the detailed experimental protocol still needs to be defined.

594 *Table 1: Summary of LS3MIP experiments. Experiments with specific treatment of subsets of*
595 *land surface features are not listed in this overview.*

Experiment ID and Tier	Experiment Description / Design	Config (L/A/O)*	Start	End	# Ens**	# Total Years**	Science Question and/or Gap Being Addressed	Synergies with other CMIP6 MIPs
Land-Hist (1)	Land only simulations	L	1850	2014	1	165	Historical land simulations	LUMIP, C4MIP, CMIP6 historical
Land-Hist-cruNcep Land-Hist-princeton Land-Hist-wfdei (2)	Land only simulations	L	1901	2014	3	342	As Land-Hist but with three different forcing data sets (Princeton forcing, CRU-NCEP, and WFDEI)	
Land-Future (2)	Land only simulations	L	2015	2100	6	516	Climate trend analysis	LUMIP, C4MIP, ScenarioMIP
LFMIP-pdLC (1)	Prescribed land conditions 1980-2014 climate	LAO	1980	2100	1	121	diagnose land-climate feedback including ocean response	ScenarioMIP
LFMIP-pdLC2 (2)	as LFMIP-pdLC with multiple model members	LAO	1980	2100	4	484	diagnose land-climate feedback including ocean response	ScenarioMIP
LFMIP-pdLC+SST (2)	Prescribed land conditions 1980-2014 climate; SSTs prescribed	LA	1980	2100	5	605	diagnose land-climate feedback over land	ScenarioMIP
LFMIP-Pobs+SST (2)	Land conditions from Land-hist; SSTs prescribed	LA	1901	2014	1	115	"perfect boundary condition" simulations	
LFMIP-rmLC (1)	Prescribed land conditions 30yr running mean	LAO	1980	2100	1	121	diagnose land-climate feedback including ocean response	ScenarioMIP
LFMIP-rmLC2 (2)	as LFMIP-rmLC with multiple model members	LAO	1980	2100	4	484	diagnose land-climate feedback including ocean response	ScenarioMIP
LFMIP-rmLC+SST (2)	Prescribed land conditions 30yr running mean; SSTs prescribed	LA	1980	2100	5	605	diagnose land-climate feedback over land	ScenarioMIP
LFMIP-Pobs (2) ^{ptbd}	Initialized pseudo-observations land	LAO	1980	2014	10	350	land-related seasonal predictability	CMIP6 historical

596 *Config L/A/O refers to land/atmosphere/ocean model configurations

597 ** # Ens refers to number of ensemble members.

598 *** # Total years is total number of simulation years.
599 ^{ptbd} experimental protocol needs to be detailed in a later stage
600

601 **Analysis strategy**

602 LS3MIP is designed to push the land surface component of climate models, observational
603 data sets and projections to a higher level of maturity. Understanding the propagation of
604 model and forecast errors and the design of model parameterizations is essential to realize
605 this goal. The LS3MIP steering group is a multi-disciplinary team (climate modellers, snow
606 and soil moisture model specialists, experts in local and remotely sensed data of soil
607 moisture and snow properties) that ensures that the experiment setups, model evaluations
608 and analyses/interpretations of the results are pertinent.

609 For both snow and soil moisture the starting point will be a careful analysis of model results
610 from on the one hand a) the DECK historic simulations (both the AMIP and the historical
611 coupled simulation) and b) on the other hand the (offline) LMIP historical simulations.

612 For the evaluation of snow representation in the models, large-scale high-quality datasets of
613 snow mass (SWE) and snow cover extent (SCE) with quantitative uncertainty characteristics
614 will be provided by the Satellite Snow Product Intercomparison and Evaluation Experiment
615 (SnowPEX¹²). Analysis within SnowPEX is providing the first evaluation of satellite derived
616 snow extent (15 participating datasets) and SWE derived from satellite measurements, land
617 surface assimilation systems, physical snow models, and reanalyses (7 participating
618 datasets). Internal consistency between products, and bias relative to independent
619 reference datasets are being derived based on standardized and consistent protocols. The
620 evaluation of variability and trends in terrestrial snow cover extent and mass was examined
621 previously for CMIP3 and CMIP5 by e.g. Brown and Mote (2009), Derksen and Brown (2012)
622 and Brutel-Vuilmet et al. (2013). While these assessments were based on single
623 observational datasets, and hence provide no perspective on observational uncertainty and
624 spread relative to multi-model ensembles, standardized multi-source datasets generated by
625 SnowPEX will allow assessment using a multi-dataset observational ensemble (e.g. Mudryk
626 et al. 2015). For snow albedo, multiple satellite-derived datasets are available, including 16-
627 day MODIS¹³ data from 2001 – present, the ESA GlobAlbedo product¹⁴, the recently updated
628 twice-daily APP-x¹⁵ product (1982 – 2011), and a derivation of the snow shortwave radiative
629 effect from 2001 – 2013 (Singh et al. 2015). Satellite retrievals of snow cover fraction in
630 forested and mountainous areas is an ongoing area of uncertainty which influences the
631 essential diagnostics related to climate sensitivity of snow cover (Thackeray et al. 2015b),

¹² <http://calvalportal.ceos.org/projects/snowpex>

¹³ <http://modis-atmos.gsfc.nasa.gov/ALBEDO/>

¹⁴ <http://www.globalbedo.org>

¹⁵ <http://stratus.ssec.wisc.edu/products/appx/appx.html>

feeding into essential diagnostics related to climate sensitivity of snow cover (Qu and Hall, 2014; Fletcher et al. 2012).

In the case of soil moisture, land hydrology and vegetation state, several observations-based datasets will be used in the evaluation of the coupled DECK simulations and offline Land experiments. Data considered will include the first multidecadal satellite-based global soil moisture record (Essential Climate Variable Soil Moisture ECVSM) (Liu et al. 2012; Dorigo et al. 2012), long-term (2002-2015) records of terrestrial water storage from the GRACE satellite (Rodell et al. 2009; Reager et al. 2016; Kim et al. 2009), the multi-product LandFlux-EVAL evapotranspiration synthesis (Mueller et al. 2013), multi-decadal satellite retrievals of the Fraction of Photosynthetically Absorbed Radiation (FPAR, e.g. Gobron et al. 2010; Zscheischler et al. 2015), and upscaled Fluxnet based products (Jung et al. 2010).

Several details of snow and soil moisture dynamical processes can be indirectly inferred through the analysis of river discharge (Orth et al. 2013; Zampieri et al. 2015). Variables simulated by the routing schemes included in the land surface models can be compared with the station data available from the Global Runoff Database (GRDC¹⁶). Combined use of in-situ discharge observations and terrestrial water storage changes observed by GRACE will verify how the land surface simulations partition the terms in the water balance equation (i.e., precipitation, evapotranspiration, runoff, and water storage changes)(Kim et al. 2009).

The coupled LS3MIP (LFMIP) simulations will be analyzed in concert with the control runs to quantify various climatic effects of snow and soil moisture, detect systematic biases and diagnose feedbacks. Anticipated analyses include:

- *Drivers of variability at multiple time scales:* comparison of simulations with prescribed soil moisture and snow (LFMIP-pdLC) allows quantification of the impact of land surface state variability on variability of climate variables such as temperature, relative humidity, cloudiness, precipitation and river discharge at several time scales. The LFMIP-rmLC simulation allows evaluation of this contribution on seasonal time scales, and changes of patterns of high/low land surface impact in a future climate. In particular, a focus will be put on impacts on climate extremes (temperature extremes, heavy precipitation events, see e.g. Seneviratne et al. 2013) and the possible role of land-based feedbacks in amplifying regional climate responses compared to changes in global mean temperature (Seneviratne et al. 2016). A secondary focus will be on the impacts of snow and soil moisture variability on the extremes of river discharge, which can be related to large-scale floods and to non-local propagation of drought signals. These aspects will be analyzed in the context of water management and to quantify feedbacks of river discharge to the climate system (through the discharge in the oceans, Materia et al. 2012; Carmack et al. 2015) and to the carbon cycle (through the methane produced in flooded areas, Meng et al. 2015)).

¹⁶ <http://www.bafg.de/GRDC>

- 670 • *Attribution of model disagreement*: the multi-model set up of the experiment allows

671 closer inspection of the effects of modeled soil moisture and snow (and related

672 processes such as plant transpiration, photosynthesis, or snowmelt) on calculated

673 land temperature, precipitation, runoff, vegetation state, and gross primary

674 production. The comparison of LFMIP-pdLC and LFMIP-rmLC will be useful to isolate

675 model disagreement in land surface feedbacks potentially induced by including

676 coupling to a dynamic ocean despite similar land response to climate change.
- 677 • *Emergent constraints*: while the annual cycle of snow cover and local temperature

678 (Qu and Hall 2014), and the relation between global mean temperature fluctuations

679 and CO₂-concentration (Cox et al. 2013) provide observational constraints on snow-

680 albedo and carbon-climate feedback respectively, similar emergent constraints may

681 be defined to constrain (regional) soil moisture or snow related feedbacks with

682 temperature or hydrological processes such as, for instance, the timing of spring

683 onset which may be related to snowmelt, spring river discharge (Zampieri et al.

684 2015) and vegetation phenology (Xu et al. 2013). Use of appropriate observations

685 and diagnostics as emergent constraints will reduce uncertainties in projections of

686 mean climate and extremes (heat extremes, droughts, floods) (Hoffman et al. 2014).

687 The analysis of amplitude and timing of seasonality of hydrological and ecosystem

688 processes will provide additional diagnostics.
- 689 • *Attribution of model bias*: a positive relationship between model temperature bias in

690 the current climate, and (regional) climate response can partly be attributed to the

691 soil moisture-climate feedback, which acts on both the seasonal and climate time

692 scale (Cheruy et al. 2014). A multi-model assessment of this relationship is enabled

693 via LS3MIP. The comparison of AMIP-DECK, LFMIP-CA and LFMIP-LCA will be used to

694 assess the impact of atmospheric-related errors in land boundary conditions on the

695 AGCM biases.
- 696 • *Changes in feedback hotspots and predictability patterns*: land surface conditions

697 don't exert uniform influence on the atmosphere in all areas of the globe: a

698 distribution of strong interaction "hotspots" and areas of high potential predictability

699 contributions from the land surface exists (e.g. Koster et al. 2004). These patterns

700 may change in a future climate (e.g. Seneviratne et al. 2006). A multi-model

701 assessment such as foreseen in LS3MIP allows mapping changes in these patterns,

702 with implications for the occurrence of droughts, heat waves, irrigation limitations or

703 river discharge anomalies and their predictability (Dirmeyer et al. 2013).
- 704 • *Snow shortwave radiative effect analysis*: The Snow Shortwave Radiative Effect

705 (SSRE) can be diagnosed through parallel calculations of surface albedo and

706 shortwave fluxes with and without model snow on the ground or in the vegetation

707 canopy (Perket et al. 2014). This metric provides a precise, overarching measure of

708 the snow-induced perturbation to solar absorption in each model, integrating over

709 the variable influences of vegetation masking, snow grain size, snow cover fraction,

soot content, etc. SSRE is analogous to the widely-used cloud radiative effect diagnostic, and its time evolution provides a measure of snow albedo feedback in the context of changing climate (Flanner et al. 2011). We recommend that the diagnostic snow shortwave radiative effect (SSRE) calculation be implemented in standard LS3MIP simulations (Tiers 1 and 2). This will enable us to evaluate the integrated effect of model snow cover on surface radiative fluxes.

- *Complementary snow-related offline experiments:* Additional offline experiments with prescribed snow albedo or snow water equivalent are planned as a follow-up to LS3MIP within the ESM-SnowMIP¹⁷ initiative. This is aimed at improving our understanding of sources of coupled model biases (global offline and site scale experiments) in order to identify priority avenues for future model development.

Regarding the snow analyses, the initial geographical focus of LS3MIP is on the continental snow cover of both hemispheres, both in ice-free areas (Northern Eurasia and North America) and on the large ice sheets (Greenland and Antarctica). Effects of snow on sea ice, and the quality of the representation of snow on sea ice in climate models, will be explored later, but is of interest because of strong recent trends of Arctic sea ice decline and the potential amplifying effect of earlier spring snow melt over land.

For soil moisture, the geographical focus is on all land areas, with special interest in agricultural locations with strong land-atmosphere interaction (transition zones between wet and dry climates), extensive irrigation areas, and high interannual variability of warm season climate in densely populated areas.

The analyses are carried out on a standardized model output data set. A summary of the requested output data is given in tables in the Annex.

Table 2: Earth System Modelling groups participating in LS3MIP

Model Name	Institute	Country
ACCESS	CSIRO/Bureau of Meteorology	Australia
ACME Land Model	U.S. Department of Energy	USA
BCC-CSM2-MR	BCC,CMA	China
CanESM	CCCma	Canada
CESM		USA
CMCC-CM2	Centro Euro-Mediterraneo sui Cambiamenti Climatici	Italy
CNRM-CM	CNRM-CERFACS	France
EC-Earth	SMHI and 26 other institutes	Sweden and 9 other European

¹⁷ <http://www.climate-cryosphere.org/activities/targeted/esm-snowmip>

		countries
FGOALS	LASG, IAP, CAS	China
GISS	NASA GISS	USA
IPSL-CM6	IPSL	France
MIROC6-CGCM	AORI, University of Tokyo / JAMSTEC / National Institute for Environmental Studies	Japan
MPI-ESM	Max Planck Institute for Meteorology (MPI-M)	Germany
MRI-ESM1.x	Meteorological Research Institute	Japan
NorESM	Norwegian Climate Service Centre	Norway
hadGEM3	Met Office	UK

Data availability

The offline forcing data for the Land-Hist experiments and output from the model simulations described in this paper will be distributed through the Earth System Grid Federation (ESGF) with digital object identifiers (DOIs) assigned. The model output required for LS3MIP is listed in the Annex. Model data distributed via ESGF will be freely accessible through data portals after registration. This infrastructure makes it possible to carry out the experiments in a distributed matter, and to allow later participation of additional modelling groups. Links to all forcings datasets will be made available via the CMIP Panel website¹⁸. Information about accreditation, data infrastructure, metadata structure, citation and acknowledging is provided by Eyring et al. (2015).

Time line, participating models and interaction strategy

The offline land surface experiments (Land-Hist) are expected to be completed in early 2017. Future time slices can only be performed when the Scenario-MIP results become available. All coupled LS3MIP simulations and their subsequent analyses will be timed after the completion of the DECK and historical 20th century simulations, expected by mid 2017. Table 2 lists the participating Earth System modelling groups.

The organisational structure of LS3MIP relies on active participation of modelling groups. Coordination structures are in place for the collection and dissemination of data and model results (Eyring et al. 2015), and for the organisation of meetings and seminars (by the core team members of LS3MIP, first six authors of this manuscript). Different from earlier experiments such as GSWP2 and GLACE1/2, no central “analysis group” is put in place that is responsible for the analyses as proposed in this manuscript. The execution and publication of analyses is considered to be a community effort of participating researchers, in order to avoid duplication of efforts and coordinate the production of scientific papers.

¹⁸ <http://www.wcrp-climate.org/index.php/wgcm-cmip/about-cmip>

Discussion: expected outcome and impact of LS3MIP

The treatment of the land surface in the current generation of climate models plays a critical role in the assessment of potential effects of widespread changes in radiative forcing, land use and biogeochemical cycles. The land surface both “receives” climatic variations (by its atmospheric forcing) and “returns” these variations as feedbacks or land surface features that are of high relevance to the people living on it. The strong coupling between land surface, atmosphere, hydrosphere and cryosphere makes an analysis of its performance characteristics challenging: the response and the state of the land surface strongly depend on the climatological context, and metrics of interactions or feedbacks, which are all difficult to define and observe (van den Hurk et al. 2011).

LS3MIP addresses these challenges by enhancing earlier diagnostic studies and experimental designs. Within the limits to which complex models such as ESMs can be evaluated with currently available observational evidence (see e.g. the interesting philosophical discussion on climate model evaluation by Lenhard and Winsberg; 2010) it will lead to enhanced understanding of the contribution of land surface treatment to overall climate model performance; give inspiration on how to optimize land surface parameterizations or their forcing; support the development of better forecasting tools, where initial conditions affect the trajectory of the forecast and can be used to optimize forecast skill; and, last but not least, provide a better historical picture of the evolution of our vital water resources during the recent century. In particular, LS3MIP will provide a solid benchmark for assessing water and climate related risks and trends therein. Given the critical importance of changes in land water availability and of impacts of changes in snow, soil moisture and land surface states for the projected evolution of climate mean and extremes, we expect that LS3MIP will help the research community make fundamental advances in this area.

Acknowledgements

The authors thank the CMIP panel of the WCRP Working Group on Climate Modelling for their efforts in coordinating the CMIP6 enterprise. G.P.W. was supported by the Joint UK DECC/Defra Met Office Hadley Climate Centre Programme (GA01101). J.M. is supported by the Biogeochemistry-Climate Feedbacks Scientific Focus Area project funded through the Regional and Global Climate Modeling Program in Climate and Environmental Sciences Division (CESD) of the Biological and Environmental Research (BER) Program in the U.S. Department of Energy (DOE) Office of Science. Oak Ridge National Laboratory is managed by UT-BATTELLE for DOE under contract DE-AC05-00OR22725. Hanna Lee (NorESM) has expressed intention to participate in LS3MIP when feasible, but has not contributed to this manuscript.

References

800 Anav, A., and Coauthors, 2013: Evaluating the Land and Ocean Components of the Global
801 Carbon Cycle in the CMIP5 Earth System Models. *J. Clim.*, **26**, 6801–6843,
802 doi:10.1175/JCLI-D-12-00417.1.

803 Baldocchi, D., and Coauthors, 2001: FLUXNET: A New Tool to Study the Temporal and Spatial
804 Variability of Ecosystem–Scale Carbon Dioxide, Water Vapor, and Energy Flux
805 Densities. *Bull. Am. Meteorol. Soc.*, **82**, 2415–2434, doi:10.1175/1520-
806 0477(2001)082<2415:FANTTS>2.3.CO;2.

807 Best, M. J., and Coauthors, 2015: The Plumbing of Land Surface Models: Benchmarking
808 Model Performance. *J. Hydrometeorol.*, **16**, 1425–1442, doi:10.1175/JHM-D-14-
809 0158.1.

810 Boone, A., and Coauthors, 2009: The AMMA Land Surface Model Intercomparison Project
811 (ALMIP). *Bull. Am. Meteorol. Soc.*, **90**, 1865–1880, doi:10.1175/2009BAMS2786.1.

812 Brown, R. D., and P. W. Mote, 2009: The Response of Northern Hemisphere Snow Cover to a
813 Changing Climate*. *J. Clim.*, **22**, 2124–2145, doi:10.1175/2008JCLI2665.1.

814 Brutel-Vuilmet, C., M. Ménégoz, and G. Krinner, 2013: An analysis of present and future
815 seasonal Northern Hemisphere land snow cover simulated by CMIP5 coupled climate
816 models. *The Cryosphere*, **7**, 67–80, doi:10.5194/tc-7-67-2013.

817 Campoy, A., A. Ducharne, F. Cheruy, F. Hourdin, J. Polcher, and J. C. Dupont, 2013: Response
818 of land surface fluxes and precipitation to different soil bottom hydrological
819 conditions in a general circulation model. *J. Geophys. Res. Atmospheres*, **118**,
820 10,725–10,739, doi:10.1002/jgrd.50627.

821 Carmack, E., and Coauthors, 2015: Fresh water and its role in the Arctic Marine System:
822 sources, disposition, storage, export, and physical and biogeochemical consequences
823 in the Arctic and global oceans. *J. Geophys. Res. Biogeosciences*, n/a – n/a,
824 doi:10.1002/2015JG003140.

825 Cattiaux, J., H. Douville, and Y. Peings, 2013: European temperatures in CMIP5: origins of
826 present-day biases and future uncertainties. *Clim. Dyn.*, **41**, 2889–2907,
827 doi:10.1007/s00382-013-1731-y.

828 Cheruy, F., J. L. Dufresne, F. Hourdin, and A. Ducharne, 2014: Role of clouds and land-
829 atmosphere coupling in midlatitude continental summer warm biases and climate
830 change amplification in CMIP5 simulations. *Geophys. Res. Lett.*, **41**, 6493–6500,
831 doi:10.1002/2014GL061145.

832 Clark, M. P., and Coauthors, 2015: Improving the representation of hydrologic processes in
833 Earth System Models. *Water Resour. Res.*, **51**, 5929–5956,
834 doi:10.1002/2015WR017096.

835 Compo, G. P., and Coauthors, 2011: The Twentieth Century Reanalysis Project. *Q. J. R.*
836 *Meteorol. Soc.*, **137**, 1–28, doi:10.1002/qj.776.

- 837 Cox, P. M., D. Pearson, B. B. Booth, P. Friedlingstein, C. Huntingford, C. D. Jones, and C. M.
838 Luke, 2013: Sensitivity of tropical carbon to climate change constrained by carbon
839 dioxide variability. *Nature*, **494**, 341–344, doi:10.1038/nature11882.
- 840 Dai, A., and K. E. Trenberth, 2002: Estimates of Freshwater Discharge from Continents:
841 Latitudinal and Seasonal Variations. *J. Hydrometeorol.*, **3**, 660–687,
842 doi:10.1175/1525-7541(2002)003<0660:EOFDfC>2.0.CO;2.
- 843 Derksen, C., and R. Brown, 2012: Spring snow cover extent reductions in the 2008–2012
844 period exceeding climate model projections. *Geophys. Res. Lett.*, **39**, L19504,
845 doi:10.1029/2012GL053387.
- 846 Dirmeyer, P. A., A. J. Dolman, and N. Sato, 1999: The Pilot Phase of the Global Soil Wetness
847 Project. *Bull. Am. Meteorol. Soc.*, **80**, 851–878, doi:10.1175/1520-
848 0477(1999)080<0851:TPPOTG>2.0.CO;2.
- 849 —, X. Gao, M. Zhao, Z. Guo, T. Oki, and N. Hanasaki, 2006: GSWP-2: Multimodel Analysis
850 and Implications for Our Perception of the Land Surface. *Bull. Am. Meteorol. Soc.*, **87**,
851 1381–1397, doi:10.1175/BAMS-87-10-1381.
- 852 —, S. Kumar, M. J. Fennessy, E. L. Altshuler, T. DelSole, Z. Guo, B. A. Cash, and D. Straus,
853 2013: Model Estimates of Land-Driven Predictability in a Changing Climate from
854 CCSM4. *J. Clim.*, **26**, 8495–8512, doi:10.1175/JCLI-D-13-00029.1.
- 855 Dirmeyer, P. A., C. Peters-Lidard, and G. Balsamo, 2015: Land-Atmosphere Interactions and
856 the Water Cycle. *Seamless prediction of the Earth system: from minutes to months*,
857 G. Brunet, S. Jones, and P.M. Ruti, Eds., Vol. No 1156 of, WMO, Geneva, p. Ch 15.
- 858 Dorigo, W., R. de Jeu, D. Chung, R. Parinussa, Y. Liu, W. Wagner, and D. Fernández-Prieto,
859 2012: Evaluating global trends (1988–2010) in harmonized multi-satellite surface soil
860 moisture. *Geophys. Res. Lett.*, **39**, n/a – n/a, doi:10.1029/2012GL052988.
- 861 Douville, Conil, Tyteca, and Voldoire, 2007: Soil moisture memory and West African
862 monsoon predictability: artefact or reality? *Clim. Dyn.*, **28**, 723–742,
863 doi:10.1007/s00382-006-0207-8.
- 864 Douville, H., 2003: Assessing the Influence of Soil Moisture on Seasonal Climate Variability
865 with AGCMs. *J. Hydrometeorol.*, **4**, 1044–1066, doi:10.1175/1525-
866 7541(2003)004<1044:ATIOSM>2.0.CO;2.
- 867 —, A. Ribes, B. Decharme, R. Alkama, and J. Sheffield, 2013: Anthropogenic influence on
868 multidecadal changes in reconstructed global evapotranspiration. *Nat. Clim Change*,
869 **3**, 59–62, doi:10.1038/nclimate1632.
- 870 —, J. Colin, E. Krug, J. Cattiaux, and S. Thao, 2016: Midlatitude daily summer temperatures
871 reshaped by soil moisture under climate change. *Geophys. Res. Lett.*, **43**, 812–818,
872 doi:10.1002/2015GL066222.

- 873 Essery, R., and Coauthors, 2009: SNOWMIP2: An Evaluation of Forest Snow Process
874 Simulations. *Bull. Am. Meteorol. Soc.*, **90**, 1120–1135,
875 doi:10.1175/2009BAMS2629.1.
- 876 Etchevers, P., and Coauthors, 2004: Validation of the energy budget of an alpine snowpack
877 simulated by several snow models (SnowMIP project). *Ann. Glaciol.*, **38**, 150–158,
878 doi:10.3189/172756404781814825.
- 879 Evans, J., F. Ji, G. Abramowitz, and M. Ekström, 2013: Optimally choosing small ensemble
880 members to produce robust climate simulations. *Environ. Res. Lett.*, **8**, 044050.
- 881 Eyring, V., S. Bony, G. A. Meehl, C. Senior, B. Stevens, R. J. Stouffer, and K. E. Taylor, 2015:
882 Overview of the Coupled Model Intercomparison Project Phase 6 (CMIP6)
883 experimental design and organisation. *Geosci Model Dev Discuss*, **2015**, 10539–
884 10583, doi:10.5194/gmdd-8-10539-2015.
- 885 Flanner, M. G., K. M. Shell, M. Barlage, D. K. Perovich, and M. A. Tschudi, 2011: Radiative
886 forcing and albedo feedback from the Northern Hemisphere cryosphere between
887 1979 and 2008. *Nat. Geosci*, **4**, 151–155, doi:10.1038/ngeo1062.
- 888 Fletcher, C. G., S. C. Hardiman, P. J. Kushner, and J. Cohen, 2009: The Dynamical Response to
889 Snow Cover Perturbations in a Large Ensemble of Atmospheric GCM Integrations. *J.*
890 *Clim.*, **22**, 1208–1222, doi:10.1175/2008JCLI2505.1.
- 891 —, H. Zhao, P. J. Kushner, and R. Fernandes, 2012: Using models and satellite observations
892 to evaluate the strength of snow albedo feedback. *J. Geophys. Res. Atmospheres*,
893 **117**, D11117, doi:10.1029/2012JD017724.
- 894 Friedlingstein, P., M. Meinshausen, V. K. Arora, C. D. Jones, A. Anav, S. K. Liddicoat, and R.
895 Knutti, 2013: Uncertainties in CMIP5 Climate Projections due to Carbon Cycle
896 Feedbacks. *J. Clim.*, **27**, 511–526, doi:10.1175/JCLI-D-12-00579.1.
- 897 Gobron, N., A. Belward, B. Pinty, and W. Knorr, 2010: Monitoring biosphere vegetation
898 1998–2009. *Geophys. Res. Lett.*, **37**, n/a – n/a, doi:10.1029/2010GL043870.
- 899 Gouttevin, I., M. Menegoz, F. Dominé, G. Krinner, C. Koven, P. Ciais, C. Tarnocai, and J.
900 Boike, 2012: How the insulating properties of snow affect soil carbon distribution in
901 the continental pan-Arctic area. *J. Geophys. Res. Biogeosciences*, **117**, n/a – n/a,
902 doi:10.1029/2011JG001916.
- 903 Gregory, J. M., and Coauthors, 2016: The Flux-Anomaly-Forced Model Intercomparison
904 Project (FAFMIP) contribution to CMIP6: Investigation of sea-level and ocean climate
905 change in response to CO₂ forcing. *Geosci Model Dev Discuss*, **2016**, 1–37,
906 doi:10.5194/gmd-2016-122.
- 907 Greve, P., B. Orlowsky, B. Mueller, J. Sheffield, M. Reichstein, and S. I. Seneviratne, 2014:
908 Global assessment of trends in wetting and drying over land. *Nat. Geosci*, **7**, 716–
909 721.

910 Griffies, S. M., and Coauthors, 2016: Experimental and diagnostic protocol for the physical
 911 component of the CMIP6 Ocean Model Intercomparison Project (OMIP). *Geosci*
 912 *Model Dev Discuss*, **2016**, 1–108, doi:10.5194/gmd-2016-77.

913 Guo, Z., and P. A. Dirmeyer, 2013: Interannual Variability of Land–Atmosphere Coupling
 914 Strength. *J. Hydrometeorol.*, **14**, 1636–1646, doi:10.1175/JHM-D-12-0171.1.

915 Haddeland, I., and Coauthors, 2011: Multimodel Estimate of the Global Terrestrial Water
 916 Balance: Setup and First Results. *J. Hydrometeorol.*, **12**, 869–884,
 917 doi:10.1175/2011JHM1324.1.

918 Hall, A., X. Qu, and J. D. Neelin, 2008: Improving predictions of summer climate change in
 919 the United States. *Geophys. Res. Lett.*, **35**, L01702, doi:10.1029/2007GL032012.

920 Hauser, M., R. Orth, and S. I. Seneviratne, subm: Role of soil moisture vs recent climate
 921 change for heat waves in western Russia. *Geophys. Res. Lett.*,.

922 Hempel, S., K. Frieler, L. Warszawski, J. Schewe, and F. Piontek, 2013: A trend-preserving
 923 bias correction – the ISI-MIP approach. *Earth Syst Dynam*, **4**, 219–236,
 924 doi:10.5194/esd-4-219-2013.

925 Hoffman, F. M., and Coauthors, 2014: Causes and implications of persistent atmospheric
 926 carbon dioxide biases in Earth System Models. *J. Geophys. Res. Biogeosciences*, **119**,
 927 141–162, doi:10.1002/2013JG002381.

928 Holland, M. M., and C. M. Bitz, 2003: Polar amplification of climate change in coupled
 929 models. *Clim. Dyn.*, **21**, 221–232, doi:10.1007/s00382-003-0332-6.

930 Hong, S.-Y., and E.-C. Chang, 2012: Spectral nudging sensitivity experiments in a regional
 931 climate model. *Asia-Pac. J. Atmospheric Sci.*, **48**, 345–355, doi:10.1007/s13143-012-
 932 0033-3.

933 van den Hurk, B., M. Best, P. Dirmeyer, A. Pitman, J. Polcher, and J. Santanello, 2011:
 934 Acceleration of Land Surface Model Development over a Decade of Glass. *Bull. Am.*
 935 *Meteorol. Soc.*, **92**, 1593–1600, doi:10.1175/BAMS-D-11-00007.1.

936 —, F. Doblas-Reyes, G. Balsamo, R. Koster, S. Seneviratne, and H. Camargo Jr, 2012: Soil
 937 moisture effects on seasonal temperature and precipitation forecast scores in
 938 Europe. *Clim. Dyn.*, **38**, 349–362, doi:10.1007/s00382-010-0956-2.

939 Jaeger, E. B., and S. I. Seneviratne, 2011: Impact of soil moisture–atmosphere coupling on
 940 European climate extremes and trends in a regional climate model. *Clim. Dyn.*, **36**,
 941 1919–1939, doi:10.1007/s00382-010-0780-8.

942 Jiafu Mao, and Coauthors, 2015: Disentangling climatic and anthropogenic controls on
 943 global terrestrial evapotranspiration trends. *Environ. Res. Lett.*, **10**, 094008.

944 Jones, C. D., and Coauthors, 2016: The C4MIP experimental protocol for CMIP6. *Geosci*
 945 *Model Dev Discuss*, **2016**, 1–52, doi:10.5194/gmd-2016-36.

946 Jung, M., and Coauthors, 2010: Recent decline in the global land evapotranspiration trend
947 due to limited moisture supply. *Nature*, **467**, 951–954, doi:10.1038/nature09396.

948 Kim, H., 2010: *Role of rivers in the spatiotemporal variations of terrestrial hydrological*
949 *circulations*. University of Tokyo,.

950 Kim, H., P. J.-F. Yeh, T. Oki, and S. Kanae, 2009: Role of rivers in the seasonal variations of
951 terrestrial water storage over global basins. *Geophys. Res. Lett.*, **36**, n/a – n/a,
952 doi:10.1029/2009GL039006.

953 Koster, R. D., M. J. Suarez, and M. Heiser, 2000: Variance and Predictability of Precipitation
954 at Seasonal-to-Interannual Timescales. *J. Hydrometeorol.*, **1**, 26–46,
955 doi:10.1175/1525-7541(2000)001<0026:VAPOPA>2.0.CO;2.

956 —, and Coauthors, 2004: Regions of Strong Coupling Between Soil Moisture and
957 Precipitation. *Science*, **305**, 1138–1140, doi:10.1126/science.1100217.

958 —, and Coauthors, 2006: GLACE: The Global Land–Atmosphere Coupling Experiment. Part
959 I: Overview. *J. Hydrometeorol.*, **7**, 590–610, doi:10.1175/JHM510.1.

960 Koster, R. D., and Coauthors, 2010a: Contribution of land surface initialization to
961 subseasonal forecast skill: First results from a multi-model experiment. *Geophys.*
962 *Res. Lett.*, **37**, L02402, doi:10.1029/2009GL041677.

963 Koster, R. D., S. P. P. Mahanama, B. Livneh, D. P. Lettenmaier, and R. H. Reichle, 2010b: Skill
964 in streamflow forecasts derived from large-scale estimates of soil moisture and
965 snow. *Nat. Geosci.*, **3**, 613–616, doi:10.1038/ngeo944.

966 Koven, C. D., W. J. Riley, and A. Stern, 2012: Analysis of Permafrost Thermal Dynamics and
967 Response to Climate Change in the CMIP5 Earth System Models. *J. Clim.*, **26**, 1877–
968 1900, doi:10.1175/JCLI-D-12-00228.1.

969 Lawrence, D. M., and Coauthors, submitted: The Land-Use Model Intercomparison Project
970 (LUMIP) experimental design. *Geosci Model Dev.*,

971 Lehning, M., 2013: Snow–atmosphere interactions and hydrological consequences. *Snow–*
972 *Atmosphere Interact. Hydrol. Consequences*, **55**, 1–3,
973 doi:10.1016/j.advwatres.2013.02.001.

974 Lenhard, J., and E. Winsberg, 2010: Holism, entrenchment, and the future of climate model
975 pluralism. *Stud. Hist. Philos. Sci. Part B*, **41**, 253–262.

976 Le Quere, C., M. R. Raupach, J. G. Canadell, and G. Marland et al., 2009: Trends in the
977 sources and sinks of carbon dioxide. *Nat. Geosci.*, **2**, 831–836, doi:10.1038/ngeo689.

978 Liu, Y. Y., W. A. Dorigo, R. M. Parinussa, R. A. M. de Jeu, W. Wagner, M. F. McCabe, J. P.
979 Evans, and A. I. J. M. van Dijk, 2012: Trend-preserving blending of passive and active
980 microwave soil moisture retrievals. *Remote Sens. Environ.*, **123**, 280–297,
981 doi:10.1016/j.rse.2012.03.014.

982 Materia, S., S. Gualdi, A. Navarra, and L. Terray, 2012: The effect of Congo River freshwater
983 discharge on Eastern Equatorial Atlantic climate variability. *Clim. Dyn.*, **39**, 2109–
984 2125, doi:10.1007/s00382-012-1514-x.

985 Meng, L., R. Paudel, P. G. M. Hess, and N. M. Mahowald, 2015: Seasonal and interannual
986 variability in wetland methane emissions simulated by CLM4Me' and CAM-chem and
987 comparisons to observations of concentrations. *Biogeosciences*, **12**, 4029–4049,
988 doi:10.5194/bg-12-4029-2015.

989 Mudryk, L. R., C. Derksen, P. J. Kushner, and R. Brown, 2015: Characterization of Northern
990 Hemisphere Snow Water Equivalent Datasets, 1981–2010. *J. Clim.*, **28**, 8037–8051,
991 doi:10.1175/JCLI-D-15-0229.1.

992 Mueller, B., and S. I. Seneviratne, 2014: Systematic land climate and evapotranspiration
993 biases in CMIP5 simulations. *Geophys. Res. Lett.*, **41**, 128–134,
994 doi:10.1002/2013GL058055.

995 —, and Coauthors, 2013: Benchmark products for land evapotranspiration: LandFlux-
996 EVAL multi-data set synthesis. *Hydrol Earth Syst Sci*, **17**, 3707–3720,
997 doi:10.5194/hess-17-3707-2013.

998 Mystakidis, S., E. L. Davin, N. Gruber, and S. I. Seneviratne, 2016: Constraining future
999 terrestrial carbon cycle projections using observation-based water and carbon flux
1000 estimates. *Glob. Change Biol.*, n/a – n/a, doi:10.1111/gcb.13217.

1001 O'Neill, B. C., and Coauthors, 2016: The Scenario Model Intercomparison Project
1002 (ScenarioMIP) for CMIP6. *Geosci Model Dev Discuss*, **2016**, 1–35, doi:10.5194/gmd-
1003 2016-84.

1004 Orth, R., and S. I. Seneviratne, submitted: Soil moisture and sea surface temperatures
1005 similarly important for land climate in the warm season in the Community Earth
1006 System Model. *J. Clim.*,.

1007 Orth, R., R. D. Koster, and S. I. Seneviratne, 2013: Inferring Soil Moisture Memory from
1008 Streamflow Observations Using a Simple Water Balance Model. *J. Hydrometeorol.*,
1009 **14**, 1773–1790, doi:10.1175/JHM-D-12-099.1.

1010 Peings, Y., H. Douville, R. Alkama, and B. Decharme, 2011: Snow contribution to springtime
1011 atmospheric predictability over the second half of the twentieth century. *Clim. Dyn.*,
1012 **37**, 985–1004, doi:10.1007/s00382-010-0884-1.

1013 Perket, J., M. G. Flanner, and J. E. Kay, 2014: Diagnosing shortwave cryosphere radiative
1014 effect and its 21st century evolution in CESM. *J. Geophys. Res. Atmospheres*, **119**,
1015 1356–1362, doi:10.1002/2013JD021139.

1016 Qu, X., and A. Hall, 2014: On the persistent spread in snow-albedo feedback. *Clim. Dyn.*, **42**,
1017 69–81, doi:10.1007/s00382-013-1774-0.

1018 Reager, J. T., A. S. Gardner, J. S. Famiglietti, D. N. Wiese, A. Eicker, and M.-H. Lo, 2016: A
 1019 decade of sea level rise slowed by climate-driven hydrology. *Science*, **351**, 699–703,
 1020 doi:10.1126/science.aad8386.

1021 Rodell, M., I. Velicogna, and J. S. Famiglietti, 2009: Satellite-based estimates of groundwater
 1022 depletion in India. *Nature*, **460**, 999–1002, doi:10.1038/nature08238.

1023 Seneviratne, S. I., D. Luthi, M. Litschi, and C. Schar, 2006: Land-atmosphere coupling and
 1024 climate change in Europe. *Nature*, **443**, 205–209, doi:10.1038/nature05095.

1025 —, T. Corti, E. L. Davin, M. Hirschi, E. B. Jaeger, I. Lehner, B. Orlowsky, and A. J. Teuling,
 1026 2010: Investigating soil moisture–climate interactions in a changing climate: A
 1027 review. *Earth-Sci. Rev.*, **99**, 125–161, doi:10.1016/j.earscirev.2010.02.004.

1028 —, and Coauthors, 2013: Impact of soil moisture-climate feedbacks on CMIP5 projections:
 1029 First results from the GLACE-CMIP5 experiment. *Geophys. Res. Lett.*, **40**,
 1030 2013GL057153, doi:10.1002/grl.50956.

1031 Seneviratne, S. I., B. Van den Hurk, D. M. Lawrence, G. Krinner, G. Hurtt, H. Kim, C. Derksen,
 1032 and et al., 2014: Land Processes, Forcings, and Feedbacks in Climate Change
 1033 Simulations: The CMIP6 “LandMIPs.” *GEWEX Newsl.*, 6–10.

1034 Seneviratne, S. I., M. G. Donat, A. J. Pitman, R. Knutti, and R. L. Wilby, 2016: Allowable CO2
 1035 emissions based on regional and impact-related climate targets. *Nature*, **529**, 477–
 1036 483.

1037 Sheffield, J., G. Goteti, and E. F. Wood, 2006: Development of a 50-Year High-Resolution
 1038 Global Dataset of Meteorological Forcings for Land Surface Modeling. *J. Clim.*, **19**,
 1039 3088–3111, doi:10.1175/JCLI3790.1.

1040 —, E. F. Wood, and M. L. Roderick, 2012: Little change in global drought over the past 60
 1041 years. *Nature*, **491**, 435–438, doi:10.1038/nature11575.

1042 Singh, D., M. G. Flanner, and J. Perket, 2015: The global land shortwave cryosphere radiative
 1043 effect during the MODIS era. *The Cryosphere*, **9**, 2057–2070, doi:10.5194/tc-9-2057-
 1044 2015.

1045 Sitch, S., and Coauthors, 2015: Recent trends and drivers of regional sources and sinks of
 1046 carbon dioxide. *Biogeosciences*, **12**, 653–679, doi:10.5194/bg-12-653-2015.

1047 Thackeray, C. W., C. G. Fletcher, and C. Derksen, 2015a: Quantifying the skill of CMIP5
 1048 models in simulating seasonal albedo and snow cover evolution. *J. Geophys. Res.*
 1049 *Atmospheres*, **120**, 5831–5849, doi:10.1002/2015JD023325.

1050 —, —, and —, 2015b: Quantifying the skill of CMIP5 models in simulating seasonal
 1051 albedo and snow cover evolution. *J. Geophys. Res. Atmospheres*, **120**, 5831–5849,
 1052 doi:10.1002/2015JD023325.

1053 Thomas, J., A. Berg, and W. Merryfield, 2015: Influence of snow and soil moisture
 1054 initialization on sub-seasonal predictability and forecast skill in boreal spring. *Clim.*
 1055 *Dyn.*, 1–17, doi:10.1007/s00382-015-2821-9.

1056 Trenberth, K. E., A. Dai, G. van der Schrier, P. D. Jones, J. Barichivich, K. R. Briffa, and J.
 1057 Sheffield, 2014: Global warming and changes in drought. *Nat. Clim Change*, **4**, 17–22.

1058 Wada, Y., L. P. Beek, F. C. Sperna Weiland, B. F. Chao, Y. Wu, and M. F. Bierkens, 2012: Past
 1059 and future contribution of global groundwater depletion to sea-level rise. *Geophys.*
 1060 *Res. Lett.*, **39**.

1061 Warszawski, L., K. Frieler, V. Huber, F. Piontek, O. Serdeczny, and J. Schewe, 2014: The Inter-
 1062 Sectoral Impact Model Intercomparison Project (ISI-MIP): Project framework. *Proc.*
 1063 *Natl. Acad. Sci.*, **111**, 3228–3232.

1064 Watanabe, S., and Coauthors, 2014: Application of performance metrics to climate models
 1065 for projecting future river discharge in the Chao Phraya River basin. *Hydrol. Res.*
 1066 *Lett.*, **8**, 33–38, doi:10.3178/hrl.8.33.

1067 Weedon, G. P., and Coauthors, 2011: Creation of the WATCH Forcing Data and Its Use to
 1068 Assess Global and Regional Reference Crop Evaporation over Land during the
 1069 Twentieth Century. *J. Hydrometeorol.*, **12**, 823–848, doi:10.1175/2011JHM1369.1.

1070 Weedon, G. P., G. Balsamo, N. Bellouin, S. Gomes, M. J. Best, and P. Viterbo, 2014: The
 1071 WFDEI meteorological forcing data set: WATCH Forcing Data methodology applied to
 1072 ERA-Interim reanalysis data. *Water Resour. Res.*, **50**, 7505–7514,
 1073 doi:10.1002/2014WR015638.

1074 Wei, Y., and Coauthors, 2014: The North American Carbon Program Multi-scale Synthesis
 1075 and Terrestrial Model Intercomparison Project – Part 2: Environmental driver data.
 1076 *Geosci Model Dev*, **7**, 2875–2893, doi:10.5194/gmd-7-2875-2014.

1077 Xu, L., and P. Dirmeyer, 2011: Snow-atmosphere coupling strength in a global atmospheric
 1078 model. *Geophys. Res. Lett.*, **38**, n/a – n/a, doi:10.1029/2011GL048049.

1079 —, and —, 2012: Snow–Atmosphere Coupling Strength. Part II: Albedo Effect Versus
 1080 Hydrological Effect. *J. Hydrometeorol.*, **14**, 404–418, doi:10.1175/JHM-D-11-0103.1.

1081 Xu, L., and Coauthors, 2013: Temperature and vegetation seasonality diminishment over
 1082 northern lands. *Nat. Clim Change*, **3**, 581–586.

1083 Yoshimura, K., and M. Kanamitsu, 2008: Dynamical Global Downscaling of Global Reanalysis.
 1084 *Mon. Weather Rev.*, **136**, 2983–2998, doi:10.1175/2008MWR2281.1.

1085 —, and —, 2013: Incremental Correction for the Dynamical Downscaling of Ensemble
 1086 Mean Atmospheric Fields. *Mon. Weather Rev.*, **141**, 3087–3101, doi:10.1175/MWR-
 1087 D-12-00271.1.

1088 Zampieri M, and Lionello P, 2011: Anthropogenic land use causes summer cooling in
1089 -Central Europe. *Clim. Res.*, **46**, 255–268.

1090 Zampieri, M., E. Serpetzoglou, E. N. Anagnostou, E. I. Nikolopoulos, and A. Papadopoulos,
1091 2012: Improving the representation of river–groundwater interactions in land
1092 surface modeling at the regional scale: Observational evidence and parameterization
1093 applied in the Community Land Model. *J. Hydrol.*, **420–421**, 72–86,
1094 doi:10.1016/j.jhydrol.2011.11.041.

1095 Zampieri, M., E. Scoccimarro, S. Gualdi, and A. Navarra, 2015: Observed shift towards earlier
1096 spring discharge in the main Alpine rivers. *Better Underst. Links Stress. Hazard*
1097 *Assess. Ecosyst. Serv. Water Scarcity*, **503–504**, 222–232,
1098 doi:10.1016/j.scitotenv.2014.06.036.

1099 Zhang, Y., and Coauthors, submitted: A Climate Data Record (CDR) for the global terrestrial
1100 water budget: 1984–2010. *J. Clim.*,.

1101 Zscheischler, J., R. Orth, and S. I. Seneviratne, 2015: A submonthly database for detecting
1102 changes in vegetation–atmosphere coupling. *Geophys. Res. Lett.*, **42**, 9816–9824,
1103 doi:10.1002/2015GL066563.

1104

1105

1106 **Annex: output data tables requested for LS3MIP**

1107

1108 *Table A1: Variable request table “LEday”: daily variables related to the energy cycle. Priority*
 1109 *index (p*) in column 1 indicates 1: “Mandatory” and 2: “Desirable”. The dimension (dim.)*
 1110 *column indicates T: time, Y: latitude, X: longitude, and Z: soil or snow layers. “Direction”*
 1111 *identifies the direction of positive numbers.*

p*	name	standard_name (cf)	long_name (netCDF)	unit	direction	dim.
1	rss	surface_net_downward_shortwave_flux	Net shortwave radiation	W/m ²	Downward	TYX
1	rls	surface_net_downward_longwave_flux	Net longwave radiation	W/m ²	Downward	TYX
2	rsds	surface_downwelling_shortwave_flux_in_air	Downward short-wave radiation	W/m ²	Downward	TYX
2	rlsds	surface_downwelling_longwave_flux_in_air	Downward long-wave radiation	W/m ²	Downward	TYX
2	rsus	surface_upwelling_shortwave_flux_in_air	Upward short-wave radiation	W/m ²	Upward	TYX
2	rlus	surface_upwelling_longwave_flux_in_air	Upward long-wave radiation	W/m ²	Upward	TYX
1	hfls	surface_upward_latent_heat_flux	Latent heat flux	W/m ²	Upward	TYX
1	hfss	surface_upward_sensible_heat_flux	Sensible heat flux	W/m ²	Upward	TYX
1	hfds	surface_downward_heat_flux	Ground heat flux	W/m ²	Downward	TYX
1	hfdsn	surface_downward_heat_flux_in_snow	Downward heat flux into snow	W/m ²	Downward	TYX
2	hfmlt	surface_snow_and_ice_melt_heat_flux	Energy of fusion	W/m ²	Soild to Liquid	TYX
2	hfsbl	surface_snow_and_ice_sublimation_heat_flux	Energy of sublimation	W/m ²	Soild to Vapor	TYX
2	tau	surface_downward_stress	Momentum flux	N/m ²	Downward	TYX
2	hfrs	temperature_flux_due_to_rainfall_expressed_as_heat_flux_onto_snow_and_ice	Heat transferred to snowpack by rainfall	W/m ²	Downward	TYX
1	dtes	change_over_time_in_thermal_energy_content_of_surface	Change in surface heat storage	J/m ²	Increase	TYX
1	dtesn	change_over_time_in_thermal_energy_content_of_surface_snow_and_ice	Change in snow/ice cold content	J/m ²	Increase	TYX
1	ts	surface_temperature	Average surface temperature	K	-	TYX
2	tsns	surface_snow_skin_temperature	Snow Surface Temperature	K	-	TYX
2	tcs	surface_canopy_skin_temperature	Vegetation Canopy Temperature	K	-	TYX
2	tgs	surface_ground_skin_temperature	Temperature of bare soil	K	-	TYX
2	tr	surface_radiative_temperature	Surface Radiative Temperature	K	-	TYX
1	albs	surface_albedo	Surface Albedo	-	-	TYX
1	albsn	snow_and_ice_albedo	Snow Albedo	-	-	TYX

1	snc	surface_snow_area_fraction	Snow covered fraction	-	-	TYX
2	albc	canopy_albedo	Canopy Albedo	-	-	TYX
2	cnc	surface_canopy_area_fraction	Canopy covered fraction	-	-	TYX
1	tsl	soil_temperature	Average layer soil temperature	K	-	TZYX
1	tsnl	snow_temperature	Temperature profile in the snow	K	-	TZYX
1	tasmax	air_temperature_maximum	Daily Maximum Near-Surface Air Temperature	K	-	TYX
1	tasmin	air_temperature_minimum	Daily Minimum Near-Surface Air Temperature	K	-	TYX
2	clt	cloud_area_fraction	Total cloud fraction	-	-	TYX

1112

Table A2: Variable request table “LWday”: daily variables related to the water cycle.

p*	name	standard_name (cf)	long_name (netCDF)	unit	direction	dim.
1	pr	precipitation_flux	Precipitation rate	kg/m ² /s	Downward	TYX
2	prra	rainfall_flux	Rainfall rate	kg/m ² /s	Downward	TYX
2	prsn	snowfall_flux	Snowfall rate	kg/m ² /s	Downward	TYX
2	prrc	convective_rainfall_flux	Convective Rainfall rate	kg/m ² /s	Downward	TYX
2	prsn	convective_snowfall_flux	Convective Snowfall rate	kg/m ² /s	Downward	TYX
1	prveg	precipitation_flux_onto_canopy	Precipitation onto canopy	kg/m ² /s	Downward	TYX
1	et	surface_evapotranspiration	Total Evapotranspiration	kg/m ² /s	Upward	TYX
1	ec	liquid_water_evaporation_flux_from_canopy	Interception evaporation	kg/m ² /s	Upward	TYX
1	tran	Transpiration	Vegetation transpiration	kg/m ² /s	Upward	TYX
1	es	liquid_water_evaporation_flux_from_soil	Bare soil evaporation	kg/m ² /s	Upward	TYX
2	eow	liquid_water_evaporation_flux_from_open_water	Open water evaporation	kg/m ² /s	Upward	TYX
2	esn	liquid_water_evaporation_flux_from_surface_snow	Snow Evaporation	kg/m ² /s	Upward	TYX
2	sbl	surface_snow_and_ice_sublimation_flux	Snow sublimation	kg/m ² /s	Upward	TYX
2	slbnosn	sublimation_amount_assuming_no_snow	Sublimation of the snow free area	kg/m ² /s	Upward	TYX
2	potet	water_potential_evapotranspiration_flux	Potential Evapotranspiration	kg/m ² /s	Upward	TYX
1	mrro	runoff_flux	Total runoff	kg/m ² /s	Out	TYX
2	mrros	surface_runoff_flux	Surface runoff	kg/m ² /s	Out	TYX
1	mrrob	subsurface_runoff_flux	Subsurface runoff	kg/m ² /s	Out	TYX
1	snm	surface_snow_and_ice_melt_flux	Snowmelt	kg/m ² /s	Solid to liquid	TYX
1	snrefr	surface_snow_and_ice_refreezing_flux	Re-freezing of water in the snow	kg/m ² /s	Liquid to solid	TYX
2	snmsl	surface_snow_melt_flux_into_soil_layer	Water flowing out of snowpack	kg/m ² /s	Out	TYX
2	qgwr	water_flux_from_soil_layer_to_groundwater	Groundwater recharge from soil layer	kg/m ² /s	Out	TYX
2	rivo	water_flux_from_upstream	River Inflow	m ³ /s	In	TYX
2	rivi	water_flux_to_downstream	River Discharge	m ³ /s	Out	TYX
1	dslw	change_over_time_in_water_content_of_soil_layer	Change in soil moisture	kg/m ²	Increase	TYX
1	dsn	change_over_time_in_surface_snow_and_ice_amount	Change in snow water equivalent	kg/m ²	Increase	TYX
1	dsw	change_over_time_in_surface_water_amount	Change in Surface Water Storage	kg/m ²	Increase	TYX
1	dcw	change_over_time_in_canopy_water_amount	Change in interception storage	kg/m ²	Increase	TYX

2	dgw	change_over_time_in_groundwater	Change in groundwater	kg/m ²	Increase	TYX
2	drivw	change_over_time_in_river_water_amount	Change in river storage	kg/m ²	Increase	TYX
1	rzwc	water_content_of_root_zone	Root zone soil moisture	kg/m ²	-	TYX
1	cw	canopy_water_amount	Total canopy water storage	kg/m ²	-	TYX
1	snw	surface_snow_amount	Snow Water Equivalent	kg/m ²	-	TZYX
1	snwc	canopy_snow_amount	SWE intercepted by the vegetation	kg/m ²	-	TYX
2	lwsnl	liquid_water_content_of_snow_layer	Liquid water in snow pack	kg/m ²	-	TZYX
1	sw	surface_water_amount_assuming_no_snow	Surface Water Storage	kg/m ²	-	TYX
1	mrlsl	moisture_content_of_soil_layer	Average layer soil moisture	kg/m ²	-	TZYX
1	mrsos	moisture_content_of_soil_layer	Moisture in top soil (10cm) layer	kg/m ²	-	TYX
1	mrsow	relative_soil_moisture_content_above_field_capacity	Total Soil Wetness	-	-	TYX
2	wtd	depth_of_soil_moisture_saturation	Water table depth	m	-	TYX
1	tw	canopy_and_surface_and_subsurface_water_amount	Terrestrial Water Storage	kg/m ²	-	TYX
2	mrlqso	mass_fraction_of_unfrozen_water_in_soil_layer	Average layer fraction of liquid moisture	-	-	TZYX
1	mrfsofr	mass_fraction_of_frozen_water_in_soil_layer	Average layer fraction of frozen moisture	-	-	TZYX
2	prrsn	mass_fraction_of_rainfall_onto_snow	Fraction of rainfall on snow.	-	-	TYX
2	prnsn	mass_fraction_of_snowfall_onto_snow	Fraction of snowfall on snow.	-	-	TYX
1	lqsn	mass_fraction_of_liquid_water_in_snow	Snow liquid fraction	-	-	TZYX
1	snd	surface_snow_thickness	Depth of snow layer	m	-	TYX
1	agesno	age_of_surface_snow	Snow Age	day	-	TYX
2	sootsn	soot_content_of_surface_snow	Snow Soot Content	kg/m ²	-	TYX
2	sic	sea_ice_area_fraction	Ice-covered fraction	-	-	TYX
2	sit	sea_ice_thickness	Sea-ice thickness	m	-	TYX
2	dfr	depth_of_frozen_soil	Frozen soil depth	m	Downward	TYX
2	dmlt	depth_of_subsurface_melting	Depth to soil thaw	m	Downward	TYX
2	tpf	permafrost_layer_thickness	Permafrost Layer Thickness	m	-	TYX
2	pflw	liquid_water_content_of_permafrost_layer	Liquid water content of permafrost layer	kg/m ²	-	TYX
			Aerodynamic conductance	m/s	-	TYX
2	ares	aerodynamic_resistance	Aerodynamic resistance	s/m	-	TYX
1	nudgincw	nudging_increment_of_total_water	Nudging Increment of Water	kg/m ²	Increase	TYX
1	hur	relative_humidity	Relative humidity	%	-	TYX
1	hurmax	relative_humidity_maximum	Daily Maximum Near-Surface Relative Humidity	%	-	TYX

1	hurmin	relative_humidity_minimum	Daily Minimum Near-Surface Relative Humidity	%	-	TYX
---	--------	---------------------------	---	---	---	-----

1114

1115 *Table A3: Variable request table “LCmon”: monthly variables related to the carbon cycle.*

P*	name	standard_name (cf)	long_name (netCDF)	unit	direction	dim.
1	gpp	gross_primary_productivity _of_carbon	Gross Primary Production	Kg/m ² /s	Downward	TYX
1	npp	net_primary_productivity_of_carbon	Net Primary Production	Kg/m ² /s	Downward	TYX
1	nep	surface_net_downward_mass_flux _of_carbon_dioxide_expressed _as_carbon_due_to _all_land_processes_excluding _anthropogenic_land_use_change	Net Ecosystem Exchange	Kg/m ² /s	Downward	TYX
1	ra	plant_respiration_carbon_flux	Autotrophic Respiration	Kg/m ² /s	Upward	TYX
1	rh	heterotrophic_respiration _carbon_flux	Heterotrophic Respiration	Kg/m ² /s	Upward	TYX
1	fLuc	surface_net_upward_mass_flux _of_carbon_dioxide_expressed _as_carbon_due_to_emission_from _anthropogenic_land_use_change	Net Carbon Mass Flux into Atmosphere due to Land Use Change	Kg/m ² /s	Upward	TYX
1	cSoil	soil_carbon_content	Carbon Mass in Soil Pool	Kg/m ²	-	TYX
1	cLitter	litter_carbon_content	Carbon Mass in Litter Pool	Kg/m ²	-	TYX
1	cVeg	vegetation_carbon_content	Carbon Mass in Vegetation	Kg/m ²	-	TYX
1	cProduct	carbon_content_of_products_of _anthropogenic_land_use_change	Carbon Mass in Products of Land Use Change	Kg/m ²	-	TYX
2	cLeaf	leaf_carbon_content	Carbon Mass in Leaves	Kg/m ²	-	TYX
2	cWood	wood_carbon_content	Carbon Mass in Wood	Kg/m ²	-	TYX
2	cRoot	root_carbon_content	Carbon Mass in Roots	Kg/m ²	-	TYX
2	cMisc	miscellaneous_living_matter _carbon_content	Carbon Mass in Other Living Compartments on Land	Kg/m ²	-	TYX
2	fVegLitter	litter_carbon_flux	Total Carbon Mass Flux from Vegetation to Litter	Kg/m ² /s	-	TYX
2	fLitterSoil	carbon_mass_flux_into_soil _from_litter	Total Carbon Mass Flux from Litter to Soil	Kg/m ² /s	-	TYX
2	fVegSoil	carbon_mass_flux_into_soil _from_vegetation_excluding_litter	Total Carbon Mass Flux from Vegetation Directly to Soil	Kg/m ² /s	-	TYX
1	treeFrac	area_fraction	Tree Cover Fraction	%	-	TYX
1	grassFrac	area_fraction	Natural Grass Fraction	%	-	TYX
1	shrubFrac	area_fraction	Shrub Fraction	%	-	TYX
1	cropFrac	area_fraction	Crop Fraction	%	-	TYX
1	pastureFrac	area_fraction	Anthropogenic Pasture Fraction	%	-	TYX

1	baresoilFrac	area_fraction	Bare Soil Fraction	%	-	TYX
1	residualFrac	area_fraction	Fraction of Grid Cell that is Land but Neither Vegetation-Covered nor Bare Soil	%	-	TYX
1	lai	leaf_area_index	Leaf Area Index	Kg/m ²	-	TYX

1116

1117 *Table A4: Variable request table “L3hr”: 3-hourly variables to generate the atmospheric*
 1118 *boundary conditions for the off-line simulation.*

p*	name	standard_name (cf)	long_name (netCDF)	unit	direction	dim.
1	rsds	surface_downwelling_shortwave_flux_in_air	Downward short-wave radiation	W/m ²	Downward	TYX
1	rlsds	surface_downwelling_longwave_flux_in_air	Downward long-wave radiation	W/m ²	Downward	TYX
1	hus	specific_humidity	Near surface specific humidity	kg/kg	-	TYX
1	ta	air_temperature	Near surface air temperature	K	-	TYX
1	ps	surface_air_pressure	Surface Pressure	Pa	-	TYX
1	ws	wind_speed	Near surface wind speed	m/s	-	TYX
2	va	northward_wind	Near surface northward wind component	m/s	Northward	TYX
2	ua	eastward_wind	Near surface eastward wind component	m/s	Eastward	TYX
2	pr	precipitation_flux	Precipitation rate	kg/m ² /s	Downward	TYX
1	prra	rainfall_flux	Rainfall rate	kg/m ² /s	Downward	TYX
1	prsn	snowfall_flux	Snowfall rate	kg/m ² /s	Downward	TYX
2	prrc	convective_rainfall_flux	Convective Rainfall rate	kg/m ² /s	Downward	TYX
2	prsnrc	convective_snowfall_flux	Convective Snowfall rate	kg/m ² /s	Downward	TYX
1	clt	cloud_area_fraction	Total cloud fraction	-	-	TYX
2	co2c	mole_fraction_of_carbon_dioxide_in_air	Near surface CO2 concentration	-	-	TYX

1119

1120

Figures

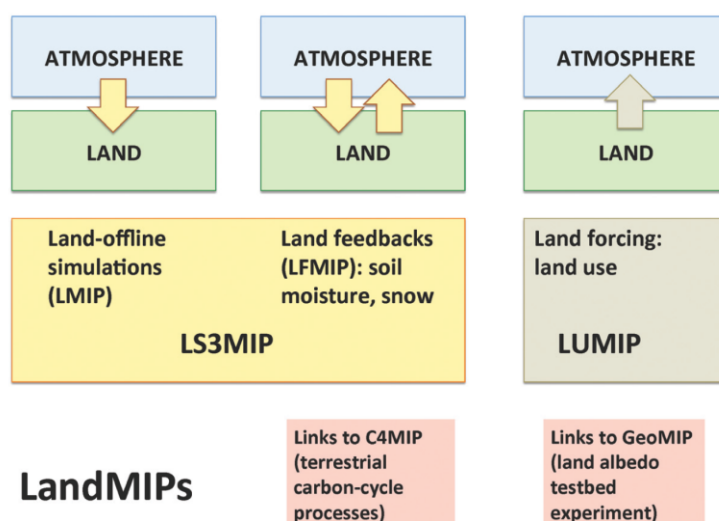


Figure 1: Structure of the “LandMIPs”. LS3MIP includes (1) the offline representation of land processes (LMIP) and (2) the representation of land-atmosphere feedbacks related to snow and soil moisture (LFMIP). Forcing associated with land use is assessed in LUMIP. Substantial links also exist to C4MIP (terrestrial carbon cycle). Furthermore, a land albedo testbed experiment is planned within GeoMIP. From Seneviratne et al. (2014)

LS3MIP within WCRP Core Projects and Grand Challenges

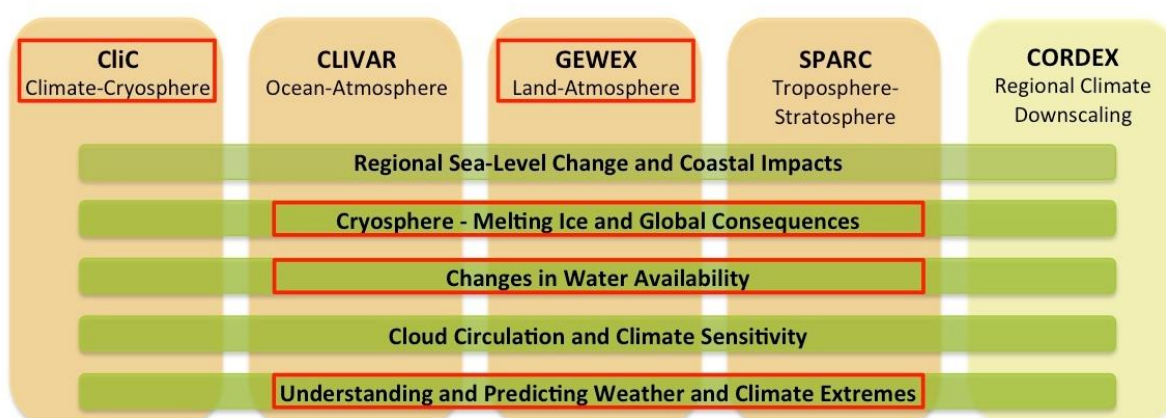


Figure 2: Relevance of LS3MIP for WCRP Core Projects and Grand Challenges¹⁹

¹⁹ <http://wcrp-climate.org/index.php/grand-challenges>; status Dec 2015

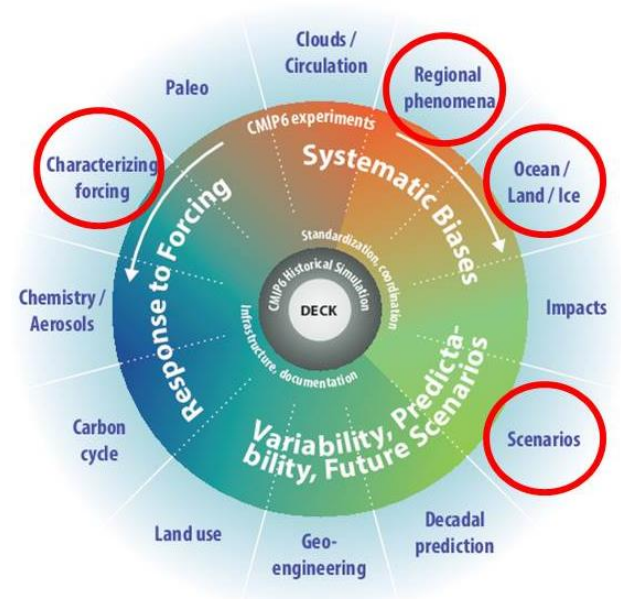


Figure 3: Embedding of LS3MIP within CMIP6. Adapted from Eyring et al. (2015)

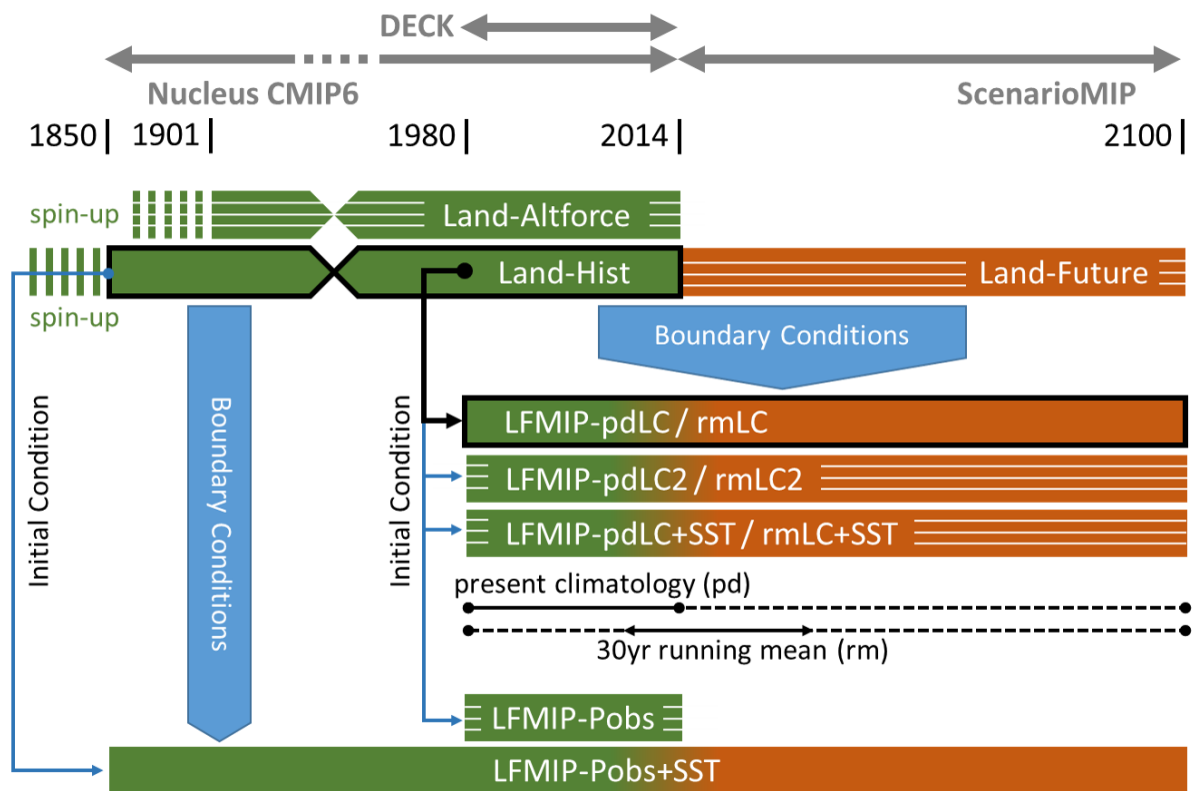


Figure 4: Schematic diagram for the experiment structure of LS3MIP. Tier 1 experiments are indicated with a heavy black outline, and complementary ensemble experiments are indicated with white hatched lines. Land-Altfrc represents 3 alternative forcings for the Land-Hist experiment. For further details on the experiments and acronyms, see Table 1 and text.

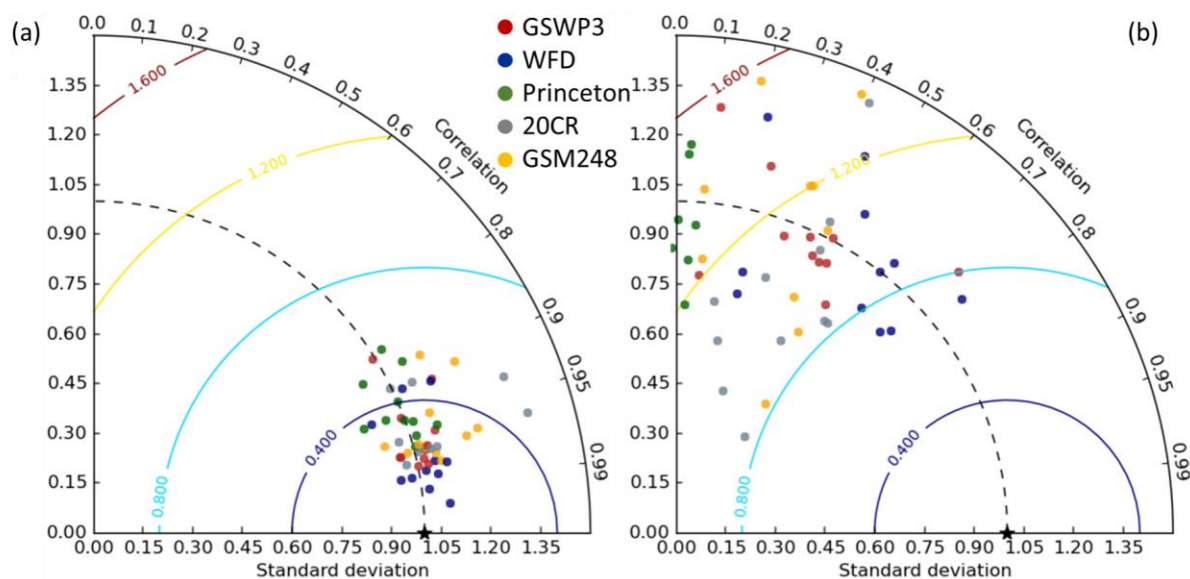


Figure 5: Taylor diagram for evaluating the forcing datasets comparing to daily observations from FLUXNET sites, as used by (Best et al. 2015): (a) 2m air temperature and (b) precipitation. Red, blue, and green dots indicate GSWP3, Watch Forcing Data (Weedon et al. 2011) and Princeton forcing (Sheffield et al. 2006), respectively. Grey and orange dots indicate 20CR and its dynamically downscaled product (GSM248).

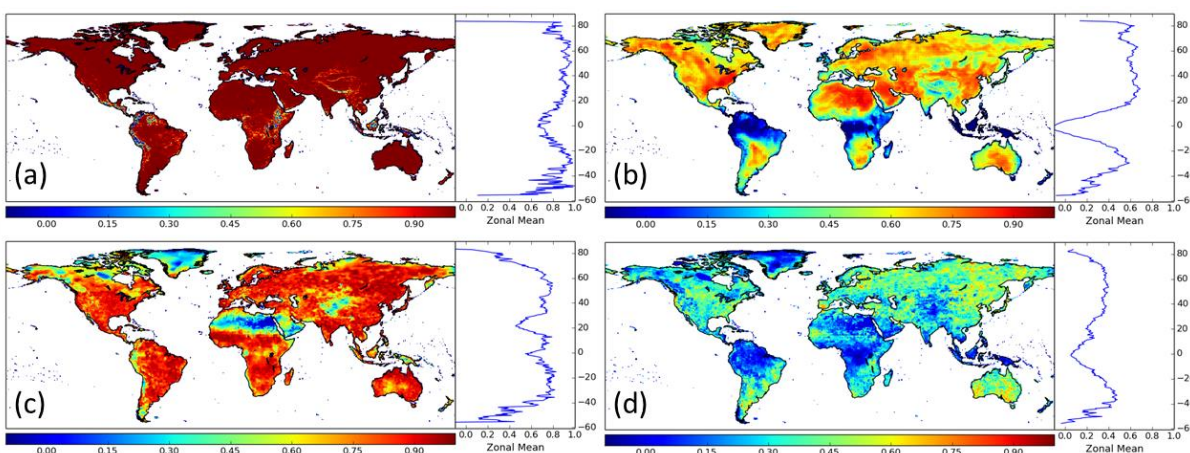


Figure 6: Global distributions of the similarity index (Ω) for 2001-2010 of monthly mean (a, c) and (b, d) monthly variance (calculated from daily data from each data set) of 2m air temperature (top panels) and precipitation (bottom panels), respectively. Shown are global distributions and zonal means. After (Kim 2010).